

From Trees to Gravity

Bergfinnur Durhuus, Thordur Jonsson and John Wheeler

Abstract In this article we study two related models of quantum geometry: generic random trees and two-dimensional causal triangulations. The Hausdorff and spectral dimensions that arise in these models are calculated and their relationship with the structure of the underlying random geometry is explored. Modifications due to interactions with matter fields are also briefly discussed. The approach to the subject is that of classical statistical mechanics and most of the tools come from probability and graph theory.

Key words: Causal triangulation, Graph theoretic, Tree correspondence, Generic trees, Spectral dimension, Hausdorff dimension, Scaling amplitude

Note This is a contribution to the *Handbook of Quantum Gravity* which will be published in the beginning of 2023. It will appear as a chapter in the section of the handbook entitled *Causal Dynamical triangulations*.

1 Introduction

In this contribution we adopt a graph theoretic and probabilistic perspective on two-dimensional Causal Dynamical Triangulations (CDTs). We consider causal triangulations (CTs) as a particular class of planar graphs (defined in Section 4.1)

Bergfinnur Durhuus

Department of Mathematical Sciences, University of Copenhagen, Universitetsparken 5, 2100 Copenhagen, Denmark, e-mail: durhuus@math.ku.dk

Thordur Jonsson

The Science Institute, University of Iceland, Dunhaga 3, 107 Reykjavik, Iceland, e-mail: thjons@hi.is

John Wheeler

Rudolf Peierls Centre for Theoretical Physics, Department of Physics, University of Oxford, Parks Road, Oxford OX1 3PU, UK, e-mail: john.wheater@physics.ox.ac.uk

that are distributed according to a probabilistic law. Our primary goal is then to apply tools from graph and probability theory to analyse the large scale geometric properties of these models. In particular we exploit, in a variety of contexts, the correspondence (established in Section 4.2) between CTs and planar tree graphs (defined in Section 3). In the process we will define and study the generic random tree model, both because of its relation to branching processes and CTs and because of its independent interest as a testing ground for investigating various aspects of random graph models in general.

We will consider two different ensembles of CTs. The first, much studied in the literature, is the grand canonical ensemble (defined in Section 5) which is based on an expansion in the size of finite graphs. We use the planar tree correspondence to give an alternative account of the scaling behaviour of loop correlation functions in the vicinity of the radius of convergence and determine the associated scaling Hausdorff dimension d_H . The second ensemble, to date less studied, is based on infinite CTs and can be thought of as an infinite volume limit suitable for studying local geometric characteristics of typical CTs. Again, we use the planar tree correspondence to investigate, in Sections 6 and 7, the fractal properties of CTs; in particular, we determine the local Hausdorff dimension d_h as well as the spectral dimension d_s (defined in Section 7.1). Indeed, for CTs all three dimension exponents, d_H , d_h and d_s have the value 2. That this is not generally the case is illustrated by the generic trees for which $d_h = d_H = 2$, but whose spectral dimension is $d_s = \frac{4}{3}$ as shown in Section 7.3.

It is obviously of interest to understand the extent to which the results outlined above are universal, and to investigate how they extend to the more general case of CTs coupled to statistical mechanical systems such as dimers and Ising spins. A few remarks on the rather sparse existing analytical results in this direction are collected in Section 8. Finally in Section 9 we draw together the possible avenues for future research.

2 Preliminary on probability

Before embarking on the main subject it is worth pointing out the difference of viewpoints represented by the two ensembles discussed above. In the grand canonical ensemble, the quantities of interest are defined as sums over graphs of finite size which are each attributed a positive finite weight. The scaling limit then involves adjusting the coupling constants so that large surfaces yield the dominant contribution to the statistical sums involved. This procedure enables the construction of the continuum limit of certain correlation functions, but does not construct the limiting distribution of continuum surfaces – although that would be an important achievement, see [1] and references therein. On the other hand, the infinite volume limit does involve the construction of a probability distribution of infinite CTs as a limit of distributions of finite CTs of fixed volume.

A simple illustration of the basic philosophy of this construction is obtained by considering standard random walk on the hypercubic integer lattice \mathbb{Z}^d . Here, a walk (or path) ω is a sequence (finite or infinite) of points $\omega_0, \omega_1, \omega_2, \dots$ in \mathbb{Z}^d such that ω_i and ω_{i+1} have distance 1 for all i . If ω consists of $N + 1$ points we say it has length N and denote it by $|\omega|$. One then attributes a weight $p(\omega) = (2d)^{-|\omega|}$ to a finite path ω starting at, say, the origin 0. Considering only paths ω of a fixed length N , the weights sum up to 1, i.e. p defines a probability distribution p_N on paths of length N . Moreover, these distributions are clearly consistent for different values of N in the sense that if $N < M$ and we consider the set consisting of all paths ω' of length M coinciding with a given path ω in the first N steps, then the weights of those paths ω' add up to $p(\omega)$. This property leads in a natural way to a probability distribution on the space of infinite paths starting at 0 as follows. Given an infinite path ω , let $\mathcal{B}_{\frac{1}{N}}(\omega)$ denote the set of finite or infinite paths coinciding with ω in the first N steps and define the probability of this set to be

$$P(\mathcal{B}_{\frac{1}{N}}(\omega)) = (2d)^{-N}.$$

Recalling that p_M attributes a weight 0 to all paths not of length M , the compatibility property implies that $P(\mathcal{B}_{\frac{1}{N}}(\omega))$ is determined by the finite size distributions as

$$P(\mathcal{B}_{\frac{1}{N}}(\omega)) = \lim_{M \rightarrow \infty} p_M(\mathcal{B}_{\frac{1}{N}}(\omega)). \quad (1)$$

It is convenient to regard $\mathcal{B}_{\frac{1}{N}}(\omega)$ as a ball of radius $\frac{1}{N}$ around ω in the space Ω of all paths (finite or infinite) starting at 0, where the distance between any two different paths ω, ω' is defined as

$$d(\omega, \omega') = \frac{1}{N + 1},$$

with $N = \max\{n \mid \omega_0 = \omega'_0, \dots, \omega_n = \omega'_n\}$. It is a consequence of a rather general result on sequences of probability measures, details of which can be found in [2], that the limiting values of ball probabilities as given by (1) uniquely specify a probability distribution on Ω , thus defining an ensemble of random paths, called random walk in \mathbb{Z}^d . By letting N grow large in the preceding discussion, it should be clear that individual paths have vanishing P -probability. Since the set of finite paths is countable, it follows that the whole set of finite paths has vanishing P -probability, which is also expressed by saying that random walks are almost surely infinite, or that P is concentrated on infinite walks. A stronger statement is that random walks are almost surely unbounded (in \mathbb{Z}^d), which we leave for the reader to figure out (it follows from the fact that random walk in a finite connected graph is recurrent, in the language of Section 7.1).

The strategy for constructing the infinite volume limit of generic trees in Section 3, and of CTs in Section 4.2, follows the procedure sketched above quite closely. It is a recurrent theme in Sections 6 and 7 to establish certain properties possessed by *typical* CTs, since the existence of atypical ones occurring with vanishing probability must be expected. A standard tool for establishing such properties is the Borel-Cantelli lemma. To formulate this result, recall first that an *event* in a probability

space Ω is simply a subset A of Ω with an associated probability $P(A) \geq 0$. In particular, $P(\Omega) = 1$ and we say that an event A occurs *almost surely* (a.s.) if $P(A) = 1$, which is equivalent to $P(\Omega \setminus A) = 0$. Moreover, probabilities of mutually exclusive events add up to the probability of their union, i.e. if A_1, A_2, \dots are events such that $A_i \cap A_j = \emptyset$ for $i \neq j$ then

$$P\left(\bigcup_i A_i\right) = \sum_i P(A_i).$$

In the example of random walk above, the set

$$E_R = \{\omega : \|\omega_n\| \leq R \text{ for all } n\},$$

where $\|\cdot\|$ denotes the Euclidean distance to the origin in \mathbb{Z}^d , is the event that a walk is confined to the ball of radius R around the origin and $\bigcup_{R=1}^{\infty} E_R$ is the event consisting of bounded walks.

Now let A_1, A_2, \dots be an arbitrary sequence of events and suppose

$$\sum_{n=1}^{\infty} P(A_n) < \infty.$$

Then, since

$$P(A_k \cup A_{k+2} \cup A_{k+3} \dots) \leq \sum_{n=k}^{\infty} P(A_n),$$

this implies that $P(A_k \cup A_{k+2} \cup A_{k+3} \dots) \rightarrow 0$ as $k \rightarrow \infty$, i.e., the probability that A_n occurs for some $n \geq k$ tends to zero as k grows large. Hence, the probability that infinitely many of the events A_n happen is 0, which is the content of the Borel-Cantelli lemma.

In our applications we typically use the Borel-Cantelli lemma to bound the size of certain graphs. For example, suppose Ω consists of infinite graphs and for any given n we associate a finite graph G_n to each $G \in \Omega$ and let $|G_n|$ denote the number of edges in G_n . If (a_n) is a sequence of positive numbers and

$$\sum_{n=1}^{\infty} P(\{G : |G_n| > a_n\}) < \infty,$$

the Borel-Cantelli lemma implies that a.s. $|G_n| > a_n$ only for a finite number of n 's and hence, $|G_n| \leq a_n$ for n large enough with probability 1.

3 Random trees

Many of the discrete structures used to model quantum gravity can be viewed as graphs or graphs with some added structure. We recall that a graph G is a set of vertices $V(G)$ and a set of edges $E(G)$ which are unordered pairs of distinct vertices. In physics applications the edges are sometimes called links. The graph is finite if the number of vertices is finite, otherwise it is infinite. The *degree* (sometimes called order or valency) of a vertex v is the number of edges containing v , which will be denoted by σ_v . We say that a graph is rooted if one vertex is singled out and called the *root*.

A *path* of length $n \geq 1$ in a graph is a sequence of oriented edges

$$(v_0, v_1), (v_1, v_2), (v_2, v_3) \dots (v_{n-1}, v_n).$$

If η is a path we use the notation $v \in \eta$ to indicate that one of the edges in η has v as an endpoint. We say that the path is *closed* if $v_0 = v_n$ and *simple* if all the vertices v_i are different except possibly v_0 and v_n which happens when the path is closed. A simple and closed path will be called a *cycle* and two cycles are considered identical if one is obtained from the other by a cyclic permutation of the edges. A trivial path consists by definition of a single vertex and is considered closed and simple and of length 0.

A graph is connected if there is a path between any two vertices. The distance (also called graph distance) between two vertices in a connected graph is the length of the shortest path connecting them. The graph spanned by a subset V_0 of vertices of a given graph G consists of V_0 itself and those edges in $E(G)$ that connect the vertices of V_0 . The ball of radius R centred at a vertex v of G is the sub-graph of G spanned by the vertices at graph distance less than or equal to R from v and will be denoted by $B_R(G; v)$. If v is the root of G the reference to v will in general be omitted. Similarly, the boundary of $B_R(G; v)$, i.e. the sub-graph spanned by the vertices at distance R from v will be called $S_R(G; v)$. The size $|G|$ of a graph G is the number of elements in $E(G)$. The number of vertices in G will be denoted $\|G\|$ and, if v is the root of G , we set $D_R(G) = \|S_R(G; v)\|$.

We define a tree to be a connected graph which does not contain any cycle. We say that a graph is planar if it is embedded in the plane such that no two edges intersect. Note that most graphs cannot be embedded in this way but all trees can and a given tree can in general be embedded in many different ways. We use the term planar tree to refer to a tree with a fixed embedding up to orientation preserving homeomorphisms of the plane. Alternatively, a planar tree can be defined as a purely combinatorial object, see e.g. [3].

3.1 The generic random tree

Let \mathcal{T} be the set of all planar rooted trees, finite or infinite, such that the root, r , is of degree 1 and all vertices have finite degree. The subset of \mathcal{T} consisting of trees of fixed size N will be denoted \mathcal{T}_N . The subset consisting of the infinite trees will be denoted \mathcal{T}_∞ . Given a tree $T \in \mathcal{T}$ and non-negative integer R , the ball $B_R(T)$ is again a rooted planar tree and its boundary $S_R(T)$ consists of $D_R(T)$ isolated vertices, whose distance R from the root will also be called their height in T . We let $T \setminus r$ denote the set of all vertices in T except the root and note that $\|T\| = |T| + 1$ for any finite tree T .

For later use we define the distance $d_{\mathcal{T}}(T, T')$ between two trees T, T' as R^{-1} , where R is the radius of the largest ball around the root common to T and T' . We can view \mathcal{T} as a metric space with metric $d_{\mathcal{T}}$, see [4] for some of its properties. In particular, for any positive integer R the ball in \mathcal{T} of radius R^{-1} is given by

$$\mathcal{B}_{\frac{1}{R}}(T) = \{T' : B_R(T') = B_R(T)\}, \quad (2)$$

i.e., it consists of all trees coinciding with T up to height R . If T has $K = D_R(T)$ vertices at height R , the trees in $\mathcal{B}_{\frac{1}{R}}(T)$ are obtained by grafting arbitrary trees T_1, \dots, T_K onto those K vertices, i.e., identifying the root edge of T_i with the edge in T incident on the i 'th vertex in $S_R(T)$. In this way, there is a one-to-one correspondence between trees in $\mathcal{B}_{\frac{1}{R}}(T)$ and K -tuples of trees in \mathcal{T} , that we shall denote by

$$F_R : \mathcal{B}_{\frac{1}{R}}(T) \rightarrow \mathcal{T}^K. \quad (3)$$

An ensemble of random graphs is a set of graphs equipped with a probability measure. In this section we define a class of ensembles of infinite trees of relevance to quantum gravity, called *generic tree ensembles*, and discuss some of their properties. We proceed by first defining probability measures on finite trees of fixed size N and then showing how to obtain a limit as N tends to infinity.

Given a set of non-negative *branching weights* w_n , $n \in \mathbb{N}$, we define, in the spirit of classical statistical mechanics, the *finite volume partition functions*, Z_N , by

$$Z_N = \sum_{T \in \mathcal{T}_N} \prod_{v \in T \setminus r} w_{\sigma_v}. \quad (4)$$

We assume $w_1 > 0$, since Z_N vanishes otherwise, and we also assume $w_n > 0$ for some $n \geq 3$ since otherwise only the linear chain of length N would contribute to Z_N . Under these assumptions the generating function ϕ for the branching weights,

$$\phi(z) = \sum_{n=1}^{\infty} w_n z^{n-1}, \quad (5)$$

is strictly increasing and strictly convex on the interval $[0, z_c)$ with $\phi(0) = w_0$, where z_c is the radius of convergence for the series (5), which we assume is positive.

It is well known, see e.g. [5], that the generating function for the finite volume partition functions,

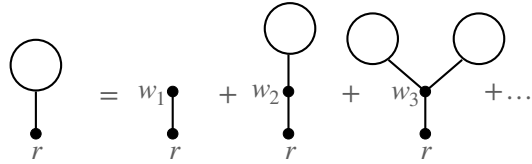
$$Z(\zeta) = \sum_{N=1}^{\infty} Z_N \zeta^N, \quad (6)$$

satisfies the equation

$$Z(\zeta) = \zeta \phi(Z(\zeta)), \quad (7)$$

where ζ is the fugacity associated to each edge. The proof of this identity is illustrated in Fig.1. If the degree of the vertex next to the root is n , then there are $n - 1$ trees attached to it in addition to the root edge, which has weight ζ . Summing over n then yields equation (7).

Fig. 1 A graphical illustration of the derivation of equation (7).



From the properties of ϕ it follows that the straight line in the plane through the origin with slope ζ^{-1} intersects the graph of ϕ at least once (and at most twice) for $\zeta > 0$ small enough, see Fig.2. By (7) and the fact that $Z(0) = 0$ it follows that $Z(\zeta)$ is determined by the first intersection point for ζ small enough and that the solution persists for $\zeta < \zeta_0$ where ζ_0 is the radius of convergence of the series (6). Since Z is an increasing function of ζ , the limit

$$Z_0 = \lim_{\zeta \uparrow \zeta_0} Z(\zeta) \quad (8)$$

is finite and $\leq z_c$. In the following we consider the *generic* case where

$$Z_0 < z_c. \quad (9)$$

In this case, it follows from (7) that the slope of the line through the origin that is tangent to the graph of ϕ equals ζ_0^{-1} , i.e. $Z_0 = Z(\zeta_0)$ is the unique positive solution to the equation

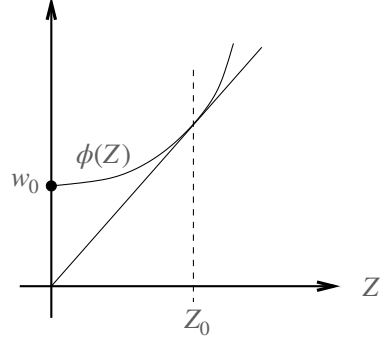
$$Z_0 \phi'(Z_0) = \phi(Z_0). \quad (10)$$

The inequality (9) is the condition on the branching weights which singles out the generic ensembles of infinite trees to be defined below. In particular, all sets of branching weights with infinite z_c define a generic ensemble.

In the special case $w_n = 1$ for all n , that will be encountered frequently in this article, we have by (4) that $Z_N = \# \mathcal{T}_N^{-1}$ and evidently $\phi(z) = (1 - z)^{-1}$ by (5). Solving

¹ We use $\#A$ to denote the number of elements in a set A .

Fig. 2 An illustration of the intersection between the graph of ϕ and a straight line through the origin in the generic case.



(7) then gives

$$Z(\zeta) = \frac{1}{2} - \frac{1}{2}\sqrt{1-4\zeta}, \quad (11)$$

so $\zeta_0 = \frac{1}{4}$ and $Z_0 = \frac{1}{2}$. Taylor expanding this expression now yields

$$Z_N = C_{N-1} := \frac{(2N-2)!}{N!(N-1)!}, \quad (12)$$

where C_N is the N th Catalan number.

Under the assumptions on the branching weights and assuming (9) we may, in the general case, Taylor expand ϕ around Z_0 in (7) and use (10) to conclude that the analytic function $Z(\zeta)$ has a square root branch point at ζ_0 and is given by

$$Z(\zeta) = Z_0 - \sqrt{\frac{2\phi(Z_0)}{\zeta_0\phi''(Z_0)}}\sqrt{\zeta_0 - \zeta} + O(\zeta_0 - \zeta), \quad (13)$$

where the square root is chosen to be positive for $\zeta < \zeta_0$. The asymptotic behaviour of Z_N is then given by

$$Z_N = \sqrt{\frac{\phi(Z_0)}{2\pi\phi''(Z_0)}} N^{-\frac{3}{2}} \zeta_0^{-N} (1 + O(N^{-1})), \quad (14)$$

provided $Z_N \neq 0$. The proof of this result can be found in [6], Sections VI.5 and VII.2. In the special case of $w_n = 1$ for all n (14) follows easily from (12) using Stirling's formula.

We define the probability distribution ν_N on \mathcal{T}_N by

$$\nu_N(T) = Z_N^{-1} \prod_{v \in T \setminus r} w_{\sigma_v}, \quad T \in \mathcal{T}_N, \quad (15)$$

assuming $Z_N \neq 0$. Using the correspondence $F_R : \mathcal{B}_{\frac{1}{R}}(T) \rightarrow \mathcal{T}^K$ described above, where $K = D_R(T)$, the probability $\nu_N(\mathcal{B}_{\frac{1}{R}}(T))$ can be expressed in terms of partition functions, and so the preceding results about the asymptotic behaviour of Z_N can be applied to determine the limiting probability as $N \rightarrow \infty$. More precisely, one obtains (see Appendix A in [7] for details)

$$\lim_{N \rightarrow \infty} \nu_N(\mathcal{B}_{\frac{1}{R}}(T)) = D_R(T) Z_0^{D_R(T)-1} \zeta_0^{|B_{R-1}(T)|} \prod_{v \in B_{R-1}(T) \setminus r} w_{\sigma_v}. \quad (16)$$

Similarly to the case of random walk in \mathbb{Z}^d discussed in Section 2, this equals the volume of $\mathcal{B}_{\frac{1}{R}}(T)$ with respect to a limit probability measure concentrated on \mathcal{T}_∞ , which we denote by ν . We call the ensembles $(\mathcal{T}_\infty, \nu)$ defined in this way *generic ensembles*, referring back to the genericity assumption (9). The expectation with respect to ν will be denoted $\langle \cdot \rangle_\nu$.

Note that if $w_n = 1$ for all n , then ν_N is the uniform measure on trees of size N , i.e.

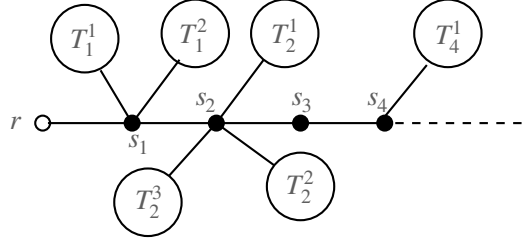
$$\nu_N(T) = \frac{1}{C_{N-1}}, \quad T \in \mathcal{T}_N. \quad (17)$$

In this case, ν is called the Uniform Infinite Planar Tree (UIPT).

The expression (16) has a simple formal interpretation which we now explain. Given an infinite tree T a *spine* for T is an infinite linear chain (non-backtracking path) in T starting at the root. We claim that ν is concentrated on the subset \mathcal{S} of \mathcal{T} consisting of trees with a single spine. Thus, if we denote the vertices on the spine by $s_0 = r, s_1, s_2, \dots$, ordered by increasing distance from the root, the trees in \mathcal{S} are obtained by attaching branches, i.e. finite trees in \mathcal{T} , to each spine vertex s_n except the root, by identifying their roots with s_n . If s_n is of degree σ there are $\sigma - 2$ branches attached to the spine at s_n . For $T \in \mathcal{S}$ we associate a weight w_{σ_v} to each vertex of T different from the root and a weight ζ_0 to each edge of T . We now argue that on a formal level these assignments characterise ν . Considering the $D_R(T) = K$ vertices of T at height $R \geq 1$, it is clear that one of them, say the i 'th from the left, must be s_R and for the corresponding K -tuple $F_R(T) = (T_1, \dots, T_K)$ this means that T_i belongs to \mathcal{S} while T_j is a finite tree in \mathcal{T} for $j \neq i$. Using the weight assignments specified above, we obtain the total weight of single spine trees in $\mathcal{B}_R(T)$ by summing over all possible K -tuples (T_1, \dots, T_K) . This yields a factor Z_0 for each $j \neq i$, while the sum over T_i is to be interpreted as an integral over \mathcal{S} with respect to ν which gives 1. Moreover, summing over the position of i yields the factor $D_R(T)$ while the remaining factors in (16) arise from the part of T below height R , thus providing the desired interpretation of (16).

Using the above description of single spine trees in terms of (finite) branches attached at spine vertices (see Fig. 3), we can obtain the probability P that the spine vertices s_1, \dots, s_n have given degrees $\sigma_1, \dots, \sigma_n$, respectively, by summing the attributed weights over the branches attached to these vertices as well as the infinite tree spanned by s_n and s_{n+1} and its descendants. Since the $\sigma_i - 2$ branches attached to s_i can be divided in $\sigma_i - 1$ ways into left and right branches and summation over individual branches yields a factor Z_0 , we obtain

Fig. 3 The first few vertices s_i on the spine of a tree and the finite branches T_i^n attached to them.



$$P = \prod_{i=1}^n \zeta_0(\sigma_i - 1) w_{\sigma_i} Z_0^{\sigma_i - 2}.$$

Noting that

$$\sum_{k=2}^{\infty} \zeta_0(k-1) w_k Z_0^{k-2} = \zeta_0 \phi'(Z_0) = 1, \quad (18)$$

where the last equality follows from (7) and (10), this shows that the degrees of spine vertices are independently and identically distributed with probability

$$\varphi(k) = \zeta_0(k-1) w_k Z_0^{k-2} \quad (19)$$

for having degree k . Similarly, it follows from the interpretation of ν just given, that the individual branches T are identically and independently distributed with probability proportional to $\zeta_0^{|T|} \prod_{v \in T \setminus r} w_{\sigma_v}$. The appropriate normalisation factor is Z_0^{-1} yielding the probability distribution

$$\mu(T) = Z_0^{-1} \zeta_0^{|T|} \prod_{v \in T \setminus r} w_{\sigma_v} \quad (20)$$

for $T \in \mathcal{T}$ finite.

Using (16) and (19) we can also determine the distribution of the total size of branches at a given spine vertex s_i , which will be needed in Section 7. Thus, denoting the union of the branches T_i^1, \dots, T_i^k at s_i by Br_i , which clearly is a tree, we define

$$\bar{Z}_N = \nu(\{|Br_i| = N\}) = \sum_{k=0}^{\infty} \sum_{N_1 + \dots + N_k = N} \varphi(k) \mu(\{|T_i^1| = N_1\}) \cdots \mu(\{|T_i^k| = N_k\}),$$

where the last equality follows from the independence of the distributions of T_i^1, \dots, T_i^k and $\varphi(k)$ is given by (19). Using also (20), the corresponding generating function is given by

$$\bar{Z}(s) = \sum_{N=0}^{\infty} \bar{Z}_N s^N = \sum_{k=0}^{\infty} \zeta_0(k+1) w_{k+2} Z(s \zeta_0)^k = \zeta_0 \phi'(Z(s \zeta_0)).$$

As before, we may use the analyticity properties of ϕ to Taylor expand the last expression around $s = 1$ and obtain

$$\bar{Z}(s) = 1 - \bar{c}_0 \sqrt{1-s} + O(|1-s|) \quad (21)$$

for s in a neighborhood of the unit circle, where $\bar{c}_0 > 0$ is a constant. Applying transfer theorems as before, see [6], this implies the asymptotic behaviour

$$\bar{Z}_N = \text{const. } N^{-3/2} \left(1 + O\left(\frac{1}{N}\right) \right).$$

for N large, which will be used in Section 7.

3.2 Trees and branching processes

We will now show how the probabilities $\mu(T)$ defined in (20) arise from a *branching process*. A Galton-Watson (GW) process is specified by a sequence p_n , $n = 0, 1, 2, \dots$, of non-negative numbers which are called *offspring probabilities* and satisfy

$$\sum_{n=0}^{\infty} p_n = 1. \quad (22)$$

The number p_n can be viewed as the probability of having n offspring. The process begins with one individual who has n offspring with probability p_n . Each of the offspring has n descendants with the same probability distribution and the process continues in the same way generation after generation. Clearly it can stop after a finite number of steps or go on for ever. The motivation of Galton and Watson was to find out how likely it was that families would die out. In order to have a one to one correspondence between trees generated by a GW process and the tree ensembles we have been discussing we have to assume that the first generation in the process has only one member since the root vertex has degree 1.

We say that the process is *critical* if the mean number of offspring is 1, i.e.,

$$\sum_{n=1}^{\infty} n p_n = 1. \quad (23)$$

A critical GW process gives rise to a probability distribution π on the subset of finite trees T in \mathcal{T} given by

$$\pi(T) = \prod_{i \in T \setminus r} p_{\sigma_i - 1} \quad (24)$$

as a consequence of (27) below. If we take

$$p_n = \zeta_0 w_{n+1} Z_0^{n-1}, \quad (25)$$

where w_n , ζ_0 and Z_0 correspond to a generic tree as described above, then

$$\sum_{n=0}^{\infty} p_n = \zeta_0 \sum_{n=0}^{\infty} w_{n+1} Z_0^{n-1} = \zeta_0 Z_0^{-1} \phi(Z_0) = 1, \quad (26)$$

where the last equality follows from (7). Furthermore, by (24) we have

$$\pi(T) = \zeta_0^{|T|} \prod_{i \in T \setminus r} w_{\sigma_i} Z_0^{\sigma_i - 2} = Z_0^{-1} \zeta_0^{|T|} \prod_{i \in T \setminus r} w_{\sigma_i} = \mu(T), \quad (27)$$

since

$$\sum_{i \in T \setminus r} (\sigma_i - 2) = -1 \quad (28)$$

for a tree T with a root of degree 1. The reader may also easily verify that (18) is equivalent to (23), so the GW process defined by (25) is critical. Note that for the uniform tree we have

$$p_n = 2^{-n-1}. \quad (29)$$

In the following we let f denote the generating function for the offspring probabilities given by (25),

$$f(s) = \sum_{n=0}^{\infty} p_n s^n = \zeta_0 \sum_{n=1}^{\infty} w_n Z_0^{n-2} s^{n-1} = \zeta_0 Z_0^{-1} \phi(Z_0 s). \quad (30)$$

Then equations (26) and (18) can be rewritten as

$$f(1) = 1 \quad \text{and} \quad f'(1) = 1. \quad (31)$$

Moreover, the genericity assumption (9) is equivalent to assuming f to be analytic in a neighbourhood of the closed unit disk.

If T is a finite tree, let $h(T)$ denote its *height*, i.e. the maximal height of vertices in T . The set of vertices at height k is called the k th generation of T and hence $D_k(T)$ is the size of the k th generation. Clearly, $D_1 = 1$ and $P(\{D_2 = n\}) = p_n$ where $P(A)$ is the probability of the event A . Let $f_n(s)$ be the generating function for D_n , i.e.,

$$f_n(s) = \sum_{k=0}^{\infty} P(\{D_n = k\}) s^k. \quad (32)$$

Then of course $f_2(s) = f(s)$. If we assume that $D_n = k$ then the probability that $D_{n+1} = q$ is given by

$$P(D_{n+1} = q \mid D_n = k) = \sum_{n_1 + n_2 + \dots + n_k = q} p_{n_1} p_{n_2} \dots p_{n_k}, \quad (33)$$

so the generating function for D_{n+1} is $f_{n+1}(s) = f(f_n(s))$. By induction it follows that f_{n+2} is the n th iterate of f .

Clearly, the average value of D_n with respect to μ equals $f'_n(1)$. By (31) it follows that $\langle D_n \rangle_\mu = 1$ for all n . As a consequence we get that

$$\langle |B_R| \rangle_\mu = \sum_{n=1}^R \langle D_n \rangle_\mu = R. \quad (34)$$

The probability that the GW process dies out, i.e., the tree has finite height, is given by

$$P(D_n = 0 \text{ for some } n) = \lim_{n \rightarrow \infty} P(D_n = 0) = \lim_{n \rightarrow \infty} f_n(0) \quad (35)$$

since $P(D_{n+1} = 0 | D_n = 0) = 1$. Since $f(0) < 1$ it is easy to see by induction that $f_n(0) < 1$ for all n . Furthermore, $f'(s) < 1$ for $0 \leq s < 1$ so $f(s) > s$ for $0 \leq s < 1$. It follows that $f_n(0)$ is increasing in n so the limit $\lim_{n \rightarrow \infty} f_n(0) = \lambda$ exists. Clearly $f(\lambda) = \lambda$ and we conclude that $\lambda = 1$, so the tree has a finite height with probability 1.

Working slightly harder one can show that

$$P(D_n > 0) = \frac{2}{nf''(1)} + O(n^{-2}), \quad (36)$$

if $f''(1)$ is finite. This means that if μ is the measure on finite trees given by (20) then

$$\mu(\{T \in \mathcal{T} : h(T) \geq R\}) = \frac{2}{f''(1)R} + O(R^{-2}) \quad (37)$$

for R large. The proof of (36) can be found, e.g., in [8].

In the special case $p_n = bc^{n-1}$ for $n \geq 1$ and $p_0 = 1 - \sum_{n \geq 1} p_n$, the proof is simple since $b = (1 - c)^2$ and

$$f(s) = \frac{c + (1 - 2c)s}{1 - cs}. \quad (38)$$

The iterates of f can be calculated explicitly:

$$f_{n+1}(s) = \frac{(n+1)c - (nc + 2c - 1)s}{1 + nc - (n+1)cs} \quad (39)$$

and

$$1 - f_{n+1}(0) = \frac{1 - c}{1 + nc}. \quad (40)$$

4 Causal triangulations

4.1 Definition

Let G be a finite rooted planar triangulation with the topology of a disk, i.e. a finite planar graph with a root S_0 such that all the faces are triangles, except one, called the *exterior face*, whose complement is a closed disk. We say that G is a *causal triangulation* (CT) if the vertices at distance k from S_0 span a cycle, i.e. the edges of $S_k(G)$ form a cycle and there are no isolated vertices in $S_k(G)$, for $0 < k < h(G)$, where

$$h(G) = \max_{v \in V(G)} d_G(S_0, v) \quad (41)$$

is called the *height* or *radius* of G . Thus, for $0 < k < h(G)$, each vertex v in $S_k(G)$ has two neighbours in $S_k(G)$ and a number $\sigma_{fv} \geq 1$ of *forward neighbours* in $S_{k+1}(G)$ as well as a number $\sigma_{bv} \geq 1$ of *of backwards neighbours* in $S_{k-1}(G)$ such that

$$\sigma_v = \sigma_{fv} + \sigma_{bv} + 2. \quad (42)$$

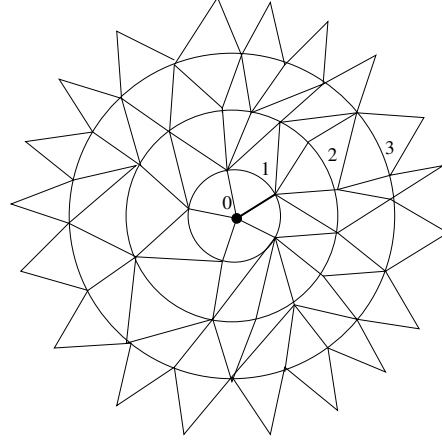
We call σ_{fv} the *forward degree* of v and σ_{bv} the *backward degree* of v , and we say v has height k in G if $v \in S_k(G)$. By convention, we shall assume that each vertex at height $h(G)$ is contained in a single triangle, thus having degree 2, and implying that boundary vertices of the disk alternate in height between $h(G)$ and $h(G) - 1$, see Fig. 4. This boundary condition is not essential to the definition of CTs but it is convenient when we come to defining the probability distributions on finite CTs below.

The preceding definition of finite CTs extends in a straightforward way to the case of infinite CTs, in which case $h(G) = \infty$ and no boundary is present. It is clear that any infinite CT can be drawn in such a way that it covers the whole plane, which we will generally assume in the following. Likewise, the definition above can easily be adapted to CTs with the topology of a cylinder that will be of interest in Section 5.

We denote by C_{fin} the collection of all finite causal triangulations of the disk; by C_{∞} the set of infinite triangulations of the plane; and by C their union. Moreover, let $C^{(h)}$ be the set consisting of CTs of height h . For technical reasons that will become clear below we will always assume that one of the edges emerging from the *central vertex* S_0 is marked and called the *root edge*. In particular, this eliminates accidental symmetries under rotations around the root vertex. An example of $G \in C^4$ is shown in Fig. 4.

We will consider two different types of ensembles of causal triangulations. In the next section the *grand canonical ensemble* based on finite CTs will be defined and associated correlation functions calculated. In the present section our main focus is on infinite CTs, making use of the results about ensembles of infinite trees in the previous section via a bijection between planar trees and CTs that we now describe.

Fig. 4 Example of $G \in \mathcal{C}^{(4)}$; the numerical labels show the heights of the cycles and the root and marked edge are shown in bold.



4.2 Bijection between CTs and planar trees

Given a causal triangulation G and $k < h(G) - 1$ we will let $\Sigma_k(G)$ denote the subgraph of G spanned by $S_k(G)$ and $S_{k+1}(G)$, i.e. it consists of the vertices in $S_k(G)$ and $S_{k+1}(G)$ together with the edges joining them. Note that $\Sigma_k(G)$ is a triangulation of an annulus for $k > 0$. Denoting by $\Delta(H)$ the number of triangles in a planar graph H , we have that

$$\Delta(\Sigma_k) = |S_k| + |S_{k+1}| \quad (43)$$

and hence, due to the chosen boundary condition, we have for $G \in \mathcal{C}_{\text{fin}}$ that

$$\Delta(G) = 2 \sum_{k=1}^{h(G)-1} |S_k(G)|. \quad (44)$$

In particular, it follows that $\Delta(G)$, which will be called the *area* of G , is even. We shall denote by \mathcal{C}_N the subset of \mathcal{C}_{fin} consisting of CTs of area $2N$ for $N \geq 1$.

Let $G \in \mathcal{C}_{\text{fin}}$. We define a planar rooted tree $T = \beta(G)$ from G in the following way:

1. The vertices of T are those of G whose height is at most $h(G) - 1$ together with a new vertex r which is the root of T and whose only neighbour is S_0 and which is placed in the triangle incident on the marked edge on the right as seen from S_0 .
2. All edges in the cycles $S_k(G)$, $k = 1, 2, \dots, h(G) - 1$, as well as those containing a vertex at maximal height are deleted, while all edges from S_0 to S_1 belong to T .
3. For each $2 \leq k < h(G) - 1$ and each vertex $v \in S_k(G)$ the rightmost of the σ_{fv} forward pointing edges as seen from v is deleted.

Conversely, let T be a rooted planar tree. Then the inverse image $G = \beta^{-1}(T)$ is obtained as follows:

- A mapping equivalent to β is described in [9]. For $G \in C_{\text{fin}}$ these mappings are variants of Schaeffer's bijection [10]. Indeed, deleting the edges in $S_k(G)$ for all k and identifying the vertices of maximal height $h(G)$ one obtains a quadrangulation to which Schaeffer's bijection can be applied; here the labelling of the vertices equals the height function. It is clear, that the bijection just described extends to the case of infinite CTs and planar trees, simply by ignoring the points pertaining to the chosen boundary condition for CTs. For an extension to more general planar quadrangulations see [3].

The diagram illustrates a spiral arrangement of triangles. A central point is labeled '0'. Three concentric circles are centered at this point. The triangles are arranged in a spiral pattern, with some triangles labeled '1', '2', and '3'.

² Note that by this convention we allow certain degenerate causal triangulations with cycles S_k having one or two edges corresponding to trees with one or two vertices at a given height.

$$d_C(G, G') = \inf\left\{\frac{1}{R+1} : B_R(G) = B_R(G')\right\}, \quad (45)$$

the map is an isometry.

Now define the uniform finite volume probability distributions ρ_N by

$$\rho_N(G) = \frac{1}{\#C_N} = \frac{1}{\#\mathcal{T}_{N+1}}, \quad G \in C_N. \quad (46)$$

Thus, we have that ρ_N is related to the uniform tree ν_N (see (17)) by

$$\rho_N(G) = \nu_N(\beta(G)), \quad G \in C_N. \quad (47)$$

It follows immediately from the existence of the UIPT ν discussed in Section 3.1 that the limit $\rho = \lim_{N \rightarrow \infty} \rho_N$ exists and is a probability measure on C_∞ given by

$$\rho(A) = \nu(\beta(A)) \quad (48)$$

for any event $A \subseteq C_\infty$.

We call the ensemble (C_∞, ρ) the *Uniform Infinite Causal Triangulation* (UIC_T). As noted in Section 3 the measure ν is concentrated on the set \mathcal{S} of single spine trees. Hence, ρ is concentrated on the subset $\beta^{-1}(\mathcal{S})$.

A result analogous to the above has been obtained for general planar triangulations in [11]. Finally, we observe that the relationship between trees and CTs described here is not the same as that introduced in [12] where the trees do not in general belong to a generic random tree ensemble.

5 Grand canonical ensemble and the scaling limit

5.1 Disk and annulus partition functions

The grand canonical ensemble for finite CTs was introduced in [13]. The disk partition function W_M for CTs of a fixed height h is defined by assigning each triangle in $G \in C^{(h)}$ (see Fig. 4) a weight g , and each boundary triangle an additional weight factor yg^{-1} ; this gives

$$\begin{aligned} W_M(g, z; h) &= \sum_{G \in C^{(h)}} |S_{h-1}(G)| (z/g)^{|S_{h-1}(G)|} g^{\Delta(G)} \\ &= z \frac{\partial}{\partial z} \sum_{G \in C^{(h)}} (z/g)^{|S_{h-1}(G)|} g^{\Delta(G)}. \end{aligned} \quad (49)$$

Here the subscript M indicates that the disk boundary is marked (recall that there is also a marked root edge), which generates the factor $|S_{h-1}(G)|$ in the weight of

G . W_M can be thought of as the discretized path integral for the amplitude that a Euclidean universe with disk topology starts at a point S_0 at Euclidean time 0, and has a single connected boundary at Euclidean time h . Then $\log g$ is the bulk cosmological constant coupled to $\Delta(G)$ which is the space time volume, and $\log y$ is the boundary cosmological constant coupled to the boundary length given by the number of boundary triangles, $|S_{h-1}(G)|$.

Correspondingly, the annulus (or cylinder) amplitude describes a Euclidean universe that evolves in Euclidean time h from an entrance boundary to an exit boundary. The contributing graphs are created from the disk graphs by inserting a second boundary at height 0; starting with $G \in C^{(h)}$ separate the triangles in Σ_0 so that they no longer have edges in common, but still have an edge in S_1 . The resulting entrance boundary contains $|S_1|$ triangles. Each is assigned an extra weight factor xg^{-1} , and one, defined to be the triangle immediately clockwise of the marked edge in G , is marked. The annulus partition function with one marked triangle on the exit boundary is then

$$W_{MM}(g, x, y; h) = \sum_{G \in C^{(h)}} (x/g)^{|S_1(G)|} |S_{h-1}(G)| (y/g)^{|S_{h-1}(G)|} g^{\Delta(G)}. \quad (50)$$

The partition functions are computed using the bijective map $\beta : C^{(h)} \rightarrow \mathcal{T}^{(h)}$ rather easily. Let $w_h(g, z)$ be the partition function for trees of height $\leq h$, with each vertex v assigned a weight $g^{2(\sigma_v-1)}$, and each vertex at height h assigned a further weight zg^{-1} , then

$$w_h(g, z) = \sum_{h' \leq h} \sum_{T \in \mathcal{T}^{(h')}} (z/g)^{\|S_h(T)\|} \left(\prod_{v \in T \setminus r} g^{2(\sigma_v-1)} \right). \quad (51)$$

Each vertex in $S_{i+1}(T)$ has exactly one edge connecting it to a vertex in $S_i(T)$ for $i = 1 \dots h(T)-1$. So every vertex $v \in T \setminus r$ contributes $\sigma_v - 1$ vertices in $G \setminus S_h(G)(G)$, where $G = \beta^{-1}(T)$, and thus, using (44),

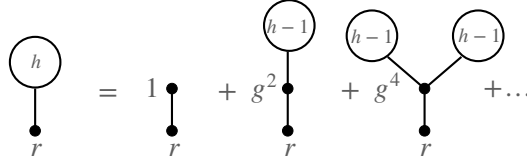
$$\Delta(G) = 2 \sum_{v \in T \setminus r} (\sigma_v - 1). \quad (52)$$

Using the map β to rewrite the right hand side of (51) as a sum over CTs gives

$$w_h(g, z) = \sum_{h' \leq h} \sum_{G \in C^{(h')}} (z/g)^{|S_{h-1}(G)|} g^{\Delta(G)}. \quad (53)$$

Only trees T of height h generate z -dependent contributions to (51), so differentiating the right hand side of (51) w.r.t. z suppresses all except the $h' = h$ terms; hence

$$z \frac{\partial}{\partial z} w_h(g, z) = W_M(g, z; h). \quad (54)$$

Fig. 6 Graphical representation of equation (55).

To compute $w_h(g, z)$ we decompose the trees of height h into trees of height $h-1$ by cutting at the vertex adjacent to the root, see Fig. 6, which gives

$$w_h(g, z) = \sum_{k=0}^{\infty} g^{2k} (w_{h-1}(g, z))^k = \frac{1}{1 - g^2 w_{h-1}(g, z)}, \quad (55)$$

with $w_1(g, z) = zg^{-1}$. This recursion is easily solved by setting $w_h = u_h/u_{h+1}$ which gives a linear difference equation for u_h ; imposing the initial condition, and choosing the convenient parametrization $g^{-1} = 2 \cosh \theta$, leads to

$$w_h(g, z) = 2 \cosh \theta \frac{\sinh(h-1)\theta - z \sinh(h-2)\theta}{\sinh h\theta - z \sinh(h-1)\theta}, \quad (56)$$

and hence the disk partition function is

$$W_M(g, z; h) = 2 \cosh \theta \frac{z \sinh^2 \theta}{(\sinh h\theta - z \sinh(h-1)\theta)^2}. \quad (57)$$

To find the annulus partition function we follow the same steps until the final iteration of the tree recurrence. Here each offspring of the vertex adjacent to the root has a weight $g^2(x/g) = xg$ instead of g^2 , so

$$\begin{aligned} W_{MM}(g, x, y; h) &= y \frac{\partial}{\partial y} \frac{1}{1 - xgw_{h-1}(g, y)} \\ &= \frac{xy \sinh^2 \theta}{(\sinh(h-1)\theta - (x+y) \sinh(h-2)\theta + xy \sinh(h-3)\theta)^2}. \end{aligned} \quad (58)$$

The partition functions (57), (58) for every h are analytic functions of g, x , and y in the region

$$A : |g| < g_c = \frac{1}{2}, \quad |x| < 1, \quad |y| < 1. \quad (59)$$

Note that for a given finite h and $g < \frac{1}{2}$ the poles of W_{MM} in x and y lie strictly outside A .

Finally, we remark that $\frac{1}{2}w_n(g = \frac{1}{2}, s)$ is the offspring probability generating function $f_{n-1}(s)$ for the uniform random tree, given by (39) with $c = \frac{1}{2}$.

5.2 Scaling amplitudes

As noted above, the partition functions (57), (58) are analytic in the region A . Within A the partition functions are dominated by graphs with small area and short boundaries. Approaching the limits of A , the area and boundary length(s) of the dominant graphs grow arbitrarily large, and the scaling limit can be constructed. Expanding (57) about $\theta = 0$ at fixed h and $y < 1$ gives

$$W_M(g, y, h) = 2 \frac{y}{(h(1-y) + y)^2} + \mathcal{O}(\theta^2), \quad (60)$$

which reflects the fact that tall trees are rare even at $g = \frac{1}{2}$. The universe described by W_M does not survive when $h \rightarrow \infty$ unless the limit is taken in such a way that $h(1-y) = \text{const}$; only then does the model generate universes which are very large, compared to the discretization scale, in the Euclidean time direction. The physically non-trivial limit is obtained by setting $g = \frac{1}{2} \text{sech } \theta$, $y = 1 - Y\theta\Lambda^{-\frac{1}{2}}$, $h = H\theta^{-1}\Lambda^{\frac{1}{2}}$ and taking $\theta \rightarrow 0$.³ The scaling amplitudes are then defined to be

$$\begin{aligned} W_M^s(\Lambda, Y, H) &= \lim_{\theta \rightarrow 0} W_M\left(\frac{1}{2} \text{sech } \theta, 1 - Y\theta\Lambda^{-\frac{1}{2}}, H\theta^{-1}\Lambda^{\frac{1}{2}}\right) \\ &= 2 \frac{\Lambda}{(\Lambda^{\frac{1}{2}} \cosh H\Lambda^{\frac{1}{2}} + Y \sinh H\Lambda^{\frac{1}{2}})^2}, \end{aligned} \quad (61)$$

and

$$\begin{aligned} W_{MM}^s(\Lambda, X, Y, H) &= \lim_{\theta \rightarrow 0} \theta^2 W_{MM}\left(\frac{1}{2} \text{sech } \theta, 1 - X\theta\Lambda^{-\frac{1}{2}}, 1 - Y\theta\Lambda^{-\frac{1}{2}}, H\theta^{-1}\Lambda^{\frac{1}{2}}\right) \\ &= \frac{\Lambda}{\left((\Lambda + XY) \sinh \Lambda^{\frac{1}{2}} H + \Lambda^{\frac{1}{2}} (X + Y) \cosh \Lambda^{\frac{1}{2}} H\right)^2}. \end{aligned} \quad (62)$$

The pre-factor θ^2 in the definition of W_{MM}^s reflects the insertion of an extra marked boundary relative to W_M^s which renders the partition function divergent at the critical point. W_M^s is the amplitude for a continuum Euclidean universe with disk topology starting at Euclidean time 0 and having a boundary at Euclidean time H with bulk cosmological constant Λ and boundary cosmological constant Y ; similarly W_{MM}^s describes a universe with, in addition, a boundary at time 0 having boundary cosmological constant X . H is chosen to have length dimension $[H] = 1$, so $[\Lambda] = -2$, and the extents of the boundaries conjugate to X and Y also have dimension 1. The scaling dimension d_H (sometimes called the scaling Hausdorff dimension) is defined through the dependence of the average area of graphs $\langle \Delta(G) \rangle_\theta$ on the height $h(\theta) = H\theta^{-1}\Lambda^{\frac{1}{2}}$ in the scaling limit of the disk ensemble

³ A mathematical treatment of the weak convergence properties of this limit is given in [14].

$$d_H = \lim_{\theta \rightarrow 0} \frac{\log \langle \Delta(G) \rangle_\theta}{\log h(\theta)}, \quad (63)$$

where

$$\langle \Delta(G) \rangle_\theta = g \frac{\partial}{\partial g} \log W_M(g, y(\theta); h(\theta)) \Big|_{g=\frac{1}{2} \operatorname{sech} \theta, y(\theta)=1-Y \theta \Lambda^{-\frac{1}{2}}}. \quad (64)$$

This gives $d_H = 2$ which is consistent with the dimension of the spatial and temporal extents each being 1, and the universes described by the scaling limit being colloquially two-dimensional. See [15] for further discussion of these partition functions.

6 Hausdorff dimension

In the previous section we introduced the dimension d_H which relates the total area and the linear extent in the limit when both become large. This section takes another point of view; we consider infinite graphs and the relation between the size of a ball and its radius as the latter becomes large.

The Hausdorff dimension d_h (sometimes called the local Hausdorff dimension) of an infinite rooted graph G is defined by the relation

$$|B_R(G)| \sim R^{d_h}, \quad R \rightarrow \infty, \quad (65)$$

where B_R as usual denotes the ball of radius R around the root and $|B_R|$ its size. More precisely, we define

$$d_h = \lim_{R \rightarrow \infty} \frac{\ln |B_R(G)|}{\ln R} \quad (66)$$

whenever the limit exists. For the ensembles of trees and surfaces that are studied here we show that this is indeed the case and yields the same value of d_h for almost all G . We shall likewise see that the same value of d_h is obtained by replacing $|B_R(G)|$ in (66) by its average value, which is in general easier to evaluate or estimate.

In many important cases $d_h = d_H$; this includes the ensembles studied in this paper, but the relation does not hold universally as will be seen in Section 8, albeit in a case where the ensemble weights may take negative values.

6.1 Generic trees

Let T be a generic tree with associated probability distribution ν . We can assume, as has been explained in Section 3, that T has a unique spine. Let T_i^n , $n = 0, 1, \dots, \sigma_{s_i} - 2$ be the finite trees attached to the i th vertex on the spine, see Fig. 3, and recall that

these are independent and each is distributed according to the probability measure μ given by (20). With notation as in Section 3.1 we have

$$Br_i = \bigcup_{n=1}^{\sigma_{s_i}-2} T_i^n, \quad (67)$$

interpreted as the empty graph if $\sigma_{s_i} = 2$. Letting Y_j denote the number of vertices different from s_i in Br_i located at distance $\leq j$ from s_i we can write

$$|B_R| = R + \sum_{i=1}^R Y_{R-i}, \quad (68)$$

where the R on the right hand side accounts for the number edges on the spine inside B_R . It follows from (19) and (25) that

$$\nu(\{\sigma_{s_i} = n + 2\}) = (n + 1)p_{n+1}. \quad (69)$$

When multiplied by n this is the $(n - 1)$ th Taylor coefficient of f'' . Using (69) and (34) this gives

$$\langle Y_{R-i} \rangle_\nu = f''(1)(R - i). \quad (70)$$

Summing over i from 1 to R yields

$$\langle |B_R| \rangle_\nu = \frac{1}{2} f''(1) R(R - 1) + R, \quad (71)$$

which shows that in terms of average values of ball sizes we have $d_h = 2$.

To obtain bounds on $|B_R(T)|$ for individual trees is more cumbersome and we shall not elaborate in detail on this issue here. In section 7.3 we show that if $G_R = \cup_{i=1}^R Br_i$ then

$$|G_R| \leq C_2 R^2 (\ln R)^3$$

holds for R large enough almost surely with respect to ν (see (110)). Since we clearly have $B_R \subseteq G_R$ the same bound holds for $|B_R|$. A similar lower bound is shown in [16] yielding the a.s. bounds

$$C_1 (\ln R)^{-2} R^2 \leq |B_R(T)| \leq C_2 R^2 (\ln R)^3, \quad (72)$$

where C_1 and C_2 are positive constants. Evidently these bounds imply that $d_h = 2$ a.s.

It is worth remarking that the ensemble average of the volume of a ball $B_R(v)$ centered at a random vertex v within some fixed distance from the root displays the same behaviour as in (72) as a simple consequence of the triangle inequality.

6.2 Causal triangulations

We now turn to the Hausdorff dimension of causal triangulations. For an infinite causal triangulation G we have

$$|B_R(G)| = 2 \sum_{i=1}^R |S_i| + \sum_{i=1}^{R-1} |S_i|, \quad (73)$$

and it follows that

$$\|B_R\| \leq |B_R| \leq 3\|B_R\|. \quad (74)$$

Clearly $\|B_R\| + 1$ equals the number of vertices within distance R from the root of the tree T corresponding to G under the bijection β . Hence, in view of (71),

$$\langle |B_R| \rangle_\rho \sim R^2, \quad R \rightarrow \infty, \quad (75)$$

where the expectation is with respect to the measure ρ defined in (48), so $d_h = 2$ for CTs. By the same argument we likewise have a.s. that

$$C'_1(\ln R)^{-2} R^2 \leq |B_R(G)| \leq C'_2 R^2 (\ln R)^3, \quad (76)$$

and hence that $d_h = 2$ a.s. with respect to ρ .

7 Spectral dimension

In this section we define a notion of dimension for graphs which is different from the ones discussed above. This is the spectral dimension which is a measure of how likely it is that a random walker returns to the starting point. In the following subsections we analyse the relation between the spectral and Hausdorff dimensions and calculate the spectral dimension for generic trees and causal triangulations.

7.1 Definition of spectral dimension of recurrent graphs

Given a graph G , we use the notation $\omega : v \rightarrow u$ to indicate a path ω from vertex v to vertex u and, if ω has length $|\omega| = m$, the vertices of ω will be denoted by $v = \omega_0, \omega_1, \dots, \omega_{m-1}, \omega_m = u$. If $v \neq u$ we write $\omega : v \rightarrow u$ for a path from v to u that does not return to v , i.e. $\omega_i \neq v$ for $i \neq 0$. If $v = u$, the notation $\omega : v \rightarrow v$ is used for a path from v to v that does not return to v in between, i.e. $\omega_i \neq v$ for $i = 1, 2, \dots, |\omega|-1$. Below we also consider infinite paths $\omega = (\omega_0\omega_1), (\omega_1\omega_2), (\omega_2\omega_3), \dots$ emerging from a vertex $v = \omega_0$.

We define the function p_G on the set of all finite paths on G by

$$p_G(\omega) = \prod_{i=0}^{|\omega|-1} \sigma_{\omega_i}^{-1}.$$

It is easily seen that p_G defines a probability distribution on the set $\Pi_m(v)$ of paths of fixed length m and fixed initial vertex v and that these distributions are compatible in the way described in Section 2. We define a probability distribution $P_{G,v}$ on the set $\Pi_\infty(v)$ of all infinite paths starting at v by setting

$$P_{G,v}(A(\bar{\omega})) = p_G(\bar{\omega}),$$

where $\bar{\omega}$ is an arbitrary finite path starting at v and $A(\bar{\omega})$ denotes the set of all infinite paths that coincide with $\bar{\omega}$ in the first $|\bar{\omega}|$ edges. When considered as probability spaces in the way described, the paths in $\Pi_m(v)$ or $\Pi_\infty(v)$ are usually referred to as *random walks*.⁴

The probability for a random walk of length m starting at v to end at u is given by

$$q_G(m; v, u) = \sum_{\omega: v \rightarrow u, |\omega|=m} p_G(\omega).$$

The corresponding *cumulative probability* is defined as

$$Q_G(n; v, u) = \sum_{m=0}^n q_G(m; v, u)$$

for any $n = 0, 1, 2, \dots$, with the convention

$$q_G(0; v, u) = \delta_{v,u} = \begin{cases} 1 & \text{if } v = u \\ 0 & \text{if } v \neq u, \end{cases}$$

i.e., we define $p_G(\omega) = 1$ for the trivial walk ω of length 0 consisting of a single vertex.

With this convention we note for later reference that Q_G fulfills

$$Q_G(n+1; v, u) = \sum_{x: (u,x) \in E(G)} \sigma_x^{-1} Q_G(n; v, x) + \delta_{v,u}, \quad n \geq 0, \quad (77)$$

where the sum on the right-hand side, as indicated, is over the neighbours of u . The quantity

$$Q'_G(n; v, u) = \sigma_u^{-1} Q_G(n; v, u),$$

which is symmetric in v and u , then fulfills the discrete version of the diffusion equation with a source at vertex v :

⁴ More commonly, they are called simple random walks, to distinguish them from, e.g., biased random walks. Since we do not consider different kinds of random walks in this paper we will leave out the adjective "simple".

$$\partial_n Q'_G(n; v, u) = -\Delta_u^G Q'_G(n; v, u) + \sigma_v^{-1} \delta_{v,u}, \quad n \geq 0, \quad (78)$$

as is easily seen by subtracting $Q_G(n; v, u)$ from both sides of equation (77). Here ∂_n denotes the difference operator with respect to "time" n and Δ^G is the graph Laplace operator acting on functions $f : V(G) \rightarrow \mathbb{C}$ according to

$$\Delta^G f(v) = \sigma_v^{-1} \sum_{x: (v,x) \in E(G)} (f(v) - f(x)).$$

The *spectral dimension* of a connected graph G is most commonly defined in terms of the decay rate of the return probability $q_G(m; v, v)$ as a function of m . More precisely, if

$$q_G(m; v, v) \sim m^{-\frac{\alpha}{2}} \quad \text{for } m \text{ large}, \quad (79)$$

we call α the spectral dimension of G and in this case G is called *recurrent* if $\alpha \leq 2$, and otherwise it is called *transient*. More generally, noting that $Q_G(n; v, v)$ is always an increasing function of n , the limit $Q_G(\infty; v, v) := \lim_{n \rightarrow \infty} Q_G(n; v, v)$ exists, and G is recurrent if the limit is ∞ , otherwise G is transient. Furthermore, we find it most convenient for our purposes to define the spectral dimension in terms of the asymptotic behaviour of $Q_G(n; v, v)$ for large n . Thus, for a recurrent graph G , we set

$$d_s = 2 - 2 \lim_{n \rightarrow \infty} \frac{\ln Q_G(n; v, v)}{\ln n}, \quad (80)$$

provided the limit exists (in which case its value is independent of v). The definition (80) is equivalent to (79) under mild assumptions.

Note that, since $1 \leq Q_G(n; v, v) \leq n$ we have $0 \leq d_s \leq 2$. Obviously, $Q_G(n; v, v)$ is not a probability, contrary to $q_G(n; v, v)$. On the other hand, letting $q_G^0(m; v, v)$ denote the first return probability after m steps of the walk, i.e.

$$q_G^0(m; v, v) = \sum_{\omega : v \rightarrow v, |\omega| = m} p_G(\omega),$$

we have that

$$Q_G^0(n; v, v) = \sum_{m=2}^n q_G^0(m; v, v)$$

is the probability that an infinite walk starting at v returns to v after at most n steps and, in particular,

$$Q_G^0(\infty; v, v) = \lim_{n \rightarrow \infty} Q_G^0(n; v, v)$$

is the probability that the infinite random walk returns at least once to v . Denoting by $\Pi_\infty^m(v)$ the set of walks that return to v at least m times we can decompose each such walk ω into pieces $\omega^{(1)}, \dots, \omega^{(m)}, \bar{\omega}$ such that $\omega^{(k)}; v \rightarrow v$ for $k = 1, 2, \dots, m$ while $\bar{\omega} \in \Pi_\infty(v)$ is an end piece. Then the set $A(\omega^{(1)}, \dots, \omega^{(m)})$ of all paths in $\Pi_\infty(v)$ whose decomposition is of the stated form with fixed $\omega_1, \dots, \omega_m$ and arbitrary $\bar{\omega}$ has probability

$$P_{G,v}(A(\omega^{(1)}, \dots, \omega^{(m)})) = P_{G,v}(A(\omega^{(1)})) \cdots P_{G,v}(A(\omega^{(m)})).$$

By summing over $\omega^{(1)}, \dots, \omega^{(m)}$ we obtain that the probability that the random walk returns at least m times to v equals $Q_G^0(\infty; v, v)^m$. Letting m tend to infinity we conclude that the probability that the random walk returns infinitely many times to the initial vertex vanishes if and only if $Q_G^0(\infty; v, v) < 1$ and the relation

$$Q_G(\infty; v, v) = \frac{1}{1 - Q_G^0(\infty; v, v)}$$

holds. On the other hand, G is recurrent if and only if $Q_G^0(\infty; v, v) = 1$ and in that case the walk returns to the initial vertex infinitely many times with probability 1. It is well known, and easy to see, that if G is finite then $d_s = 0$ while if G is the hypercubic lattice \mathbb{Z}^d (viewed as a graph in the standard way) it is a classical result of Polya, see, e.g., Ch.2 in [17], that G is recurrent if and only if $d \leq 2$, and in all cases $d_s = d$. In this article we are mainly concerned with recurrent graphs.

7.2 Relation between d_s and d_h

We now give an elementary proof of a well known inequality between the spectral dimension and the Hausdorff dimension d_h valid for arbitrary recurrent graphs. This inequality has been proven under certain assumptions on the behaviour of the volume of balls under scaling in [18, 19]. Related results for Riemannian manifolds were obtained earlier under similar assumptions in [20]. Here we essentially need no assumptions beyond existence of d_s and d_h . Specifically, we now show that if G is a connected recurrent graph such that d_s and d_h both exist, then

$$d_s \geq \frac{2d_h}{1 + d_h}. \quad (81)$$

The proof is based on a simple observation whose formulation requires some further notation. Thus, let G_0 be a subgraph of a graph G . The *inner boundary* $\partial_{in} G_0$ of G_0 is the subgraph of G spanned by the vertices of G_0 having at least one neighbour in $V(G) \setminus V(G_0)$. Similarly, the *outer boundary* $\partial_{out} G_0$ is the subgraph of G spanned by the vertices not in G_0 having at least one neighbour in G_0 . The closure $\overline{G_0}$ of G_0 is the subgraph spanned by the vertices of G_0 and those of $\partial_{out} G_0$. The *out-degree* σ_v^{out} of a vertex v in G_0 is by definition the number of neighbours of v in G that do not belong to G_0 . In particular, a vertex of G_0 belongs to $\partial_{in} G_0$ if and only if its out-degree is positive.

Now, let G be a connected graph, V_0 a proper subset of $V(G)$, and denote by G_0 the subgraph of G spanned by V_0 . Then, for arbitrary fixed $v_0 \in V_0$, we have

$$\sum_{v \in \partial_{in} G_0} \sum_{\substack{\omega: v_0 \rightarrow v \\ \omega \subseteq G_0}} p_G(\omega) \sigma_v^{-1} \sigma_v^{out} \leq 1, \quad (82)$$

with equality holding if \bar{G}_0 is connected and recurrent.

The inequality (82) follows by observing that the left-hand side is the probability q with respect to P_{G,v_0} that a walk starting at v_0 leaves G_0 . In fact, given such a walk $\tilde{\omega}$ let v denote the last vertex in G_0 visited by $\tilde{\omega}$ before it leaves G_0 for the first time and let ω denote the corresponding initial part of $\tilde{\omega}$ from v_0 to v contained in G_0 . Then $v \in \partial_{in} G_0$ and there are σ_v^{out} vertices in \bar{G}_0 that $\tilde{\omega}$ may hit next with each such possibility contributing a probability $p_G(\omega)\sigma_v^{-1}$ to q . This proves (82). Clearly, q only depends on \bar{G}_0 and if this graph is connected and recurrent it is well known [21] that the probability for a walk to hit any given vertex of \bar{G}_0 equals 1. In particular, since $V_0 \neq V(G)$, it follows that $q = 1$.

For use in the proof of (81) we note two useful consequences of (82). First, let G be a connected graph and let v_0 and u_0 be two different vertices of G . Then

$$\sum_{\substack{\omega: v_0 \rightarrow v_0 \\ u_0 \in \omega}} p_G(\omega) \leq \sigma_{v_0} \sigma_{u_0}^{-1} \sum_{\omega: v_0 \rightarrow u_0} p_G(\omega), \quad (83)$$

and equality holds if G is recurrent.

To prove this statement we set $V_0 = V(G) \setminus \{u_0\}$ and let G_0 be the sub-graph of G spanned by V_0 . In other words, G_0 is obtained from G by removing u_0 and the edges containing u_0 , and is frequently denoted by $G - u_0$. Now note that $v_0 \in G_0$ and that every walk $\omega: v_0 \rightarrow v_0$ containing u_0 can be decomposed uniquely into a walk $\omega': v_0 \rightarrow u_0$ and a walk $\omega'': u_0 \rightarrow v_0$, such that ω'' does not return to u_0 . Hence, the reverse of ω'' is a walk ω''' in G_0 from v_0 to some $v \in \partial_{in} G_0$ and one additional step to u_0 . Since $\sigma_v^{out} = 1$ for all $v \in \partial_{in} G_0$ in this case, (82) gives

$$\begin{aligned} \sum_{\substack{\omega: v_0 \rightarrow v_0 \\ u_0 \in \omega}} p_G(\omega) &= \sum_{\omega': v_0 \rightarrow u_0} p_G(\omega') \sigma_{u_0}^{-1} \sum_{v \in \partial_{in} G_0} \sum_{\substack{\omega'': v_0 \rightarrow v \\ \omega'' \subseteq G_0}} p_G(\omega'') \sigma_v^{-1} \sigma_{v_0} \\ &\leq \sum_{\omega': v_0 \rightarrow u_0} \sigma_{v_0} \sigma_{u_0}^{-1} p_G(\omega'), \end{aligned}$$

with equality holding if G is recurrent. This proves (83).

Second, with G and v_0 and u_0 as above we have that

$$\sum_{\substack{\omega: v_0 \rightarrow v_0 \\ u_0 \notin \omega}} p_G(\omega) \leq \sigma_{v_0} d_G(v_0, u_0). \quad (84)$$

In order to verify this claim, let $(v_0 v_1), (v_1 v_2), \dots, (v_{N-2} v_{N-1}), (v_{N-1} u_0)$ be a path from v_0 to u_0 of minimal length $N = d_G(v_0, u_0)$. Set $v_N = u_0$ and define k_ω , for each walk $\omega: v_0 \rightarrow v_0$, to be the maximal index k such that $v_k \in \omega$. In particular, if $u_0 \notin \omega$ then $k_\omega \leq N - 1$ and

$$v_{k_\omega} \in \omega, \quad v_{k_\omega+1}, \dots, v_N \notin \omega.$$

Given that $k_\omega = l \geq 1$ there is a unique decomposition of ω into a walk $\omega': v_0 \rightarrow v_l$ and a walk $\omega'': v_l \rightarrow v_0$ such that ω'' does not return to v_l . As previously, the

reverse of ω'' is a walk ω''' from v_0 to a neighbour v of v_l avoiding v_l, v_{l+1}, \dots, v_N , and an additional last step from v to v_l . Setting $V_0 = V(G) \setminus \{v_l, \dots, v_N\}$ and $V_1 = V(G) \setminus \{v_{l+1}, \dots, v_N\}$ and letting G_0 and G_1 be the subgraphs of G spanned by V_0 and V_1 , respectively, it follows that $\omega' \subseteq G_1$ and $\omega''' \subseteq G_0$. Noting that $v \in \partial_{in} G_0$ and that

$$p_G(\omega) = p_G(\omega') \sigma_{v_l}^{-1} \sigma_{v_0} p_G(\omega''') \sigma_v^{-1}$$

we conclude that

$$\sum_{\substack{\omega: v_0 \rightarrow v_0 \\ k_\omega = l}} p_G(\omega) \leq \sigma_{v_0} \left(\sum_{\substack{\omega': v_0 \rightarrow v_l \\ \omega' \subseteq G_1}} p_G(\omega') \sigma_{v_l}^{-1} \right) \left(\sum_{v \in \partial_{in} G_0} \sum_{\substack{\omega''': v_0 \rightarrow v \\ \omega''' \subseteq G_0}} p_G(\omega''') \sigma_v^{-1} \right). \quad (85)$$

Since $v_l \in \partial_{in} G_1$ it follows from (82) that the expressions in parentheses on the right-hand side are bounded by 1 such that

$$\sum_{\substack{\omega: v_0 \rightarrow v_0 \\ k_\omega = l}} p_G(\omega) \leq \sigma_{v_0}. \quad (86)$$

In the case $k_\omega = 0$ the walk ω'' is trivial and the reader easily verifies that the above inequality still holds with the trivial walk also included on the left-hand side contributing 1 to the sum. Finally, summing on both sides of (86) from $l = 0$ to $l = N - 1$, the claimed inequality (84) follows.

We are now ready to give a proof of (81). Let $v_0 \in G$ be fixed. Since p_G is a probability distribution on walks of length m starting at v_0 , the identity

$$\sum_{v \in G} Q_G(n; v_0, v) = \sum_{v \in G} \sum_{\substack{\omega: v_0 \rightarrow v \\ |\omega| \leq n}} p_G(\omega) = n + 1 \quad (87)$$

holds for each $n \geq 0$. Restricting the sum on the left-hand side to vertices in $B_R(G; v_0)$ we obtain an inequality instead, which implies that there exists a vertex $v_{R,n}$ in $B_R(G; v_0)$ such that

$$Q_G(n; v_0, v_{R,n}) \leq \frac{n + 1}{\|B_R(G; v_0)\|}, \quad (88)$$

where R is an arbitrary positive integer. Writing

$$Q_G(n; v_0, v_0) = \sum_{\substack{\omega: v_0 \rightarrow v_0 \\ v_{R,n} \in \omega, |\omega| \leq n}} p_G(\omega) + \sum_{\substack{\omega: v_0 \rightarrow v_0 \\ v_{R,n} \notin \omega, |\omega| \leq n}} p_G(\omega),$$

it follows from (83) and (84) together with (88) that

$$\begin{aligned}
Q_G(n; v_0, v_0) &\leq \sigma_{v_0} \sigma_{v_{R,n}}^{-1} \sum_{\substack{\omega: v_0 \rightarrow v_{R,n} \\ |\omega| \leq n}} p_G(\omega) + \sigma_{v_0} d_G(v_0, v_{R,n}) \\
&\leq \sigma_{v_0} Q_G(n; v_0, v_{R,n}) + \sigma_{v_0} d_G(v_0, v_{R,n}) \\
&\leq \sigma_{v_0} \left(\frac{n+1}{\|B_R(G; v_0)\|} + R \right). \tag{89}
\end{aligned}$$

Now, choose R as a function of n such that the two terms in parenthesis are of the same order of magnitude. This is obtained for $R = \lfloor n^{\frac{1}{1+d_h}} \rfloor$, where $\lfloor a \rfloor$ denotes the integer part of the real number a . In this case, the inequality (89) gives

$$\frac{\ln Q_G(n; v_0, v_0)}{\ln n} \leq \frac{1}{1+d_h} + \frac{\ln \sigma_{v_0} + \ln \left(1 + \frac{n+1}{R \|B_R(G; v_0)\|} \right)}{\ln n}.$$

Here, the last term tends to zero as $n \rightarrow \infty$ by the assumption that d_h exists and hence, by (80), we get

$$d_s \geq 2 - 2 \frac{1}{1+d_h} = \frac{2d_h}{1+d_h}$$

as desired.

7.3 Spectral dimension of generic trees

For the generic trees we noted in Section 6 that $d_h = 2$ with probability 1. Hence, it follows from (81) that

$$d_s \geq \frac{4}{3} \tag{90}$$

with probability 1, provided the limit (80) exists. We do not provide detailed arguments for the existence of the limit, but some further comments on this issue can be found at the end of this subsection. Next, we aim at proving that equality holds in (90) and for that we need a suitable lower bound on $Q(n; v_0, v_0)$ supplementing the upper bound (89).

In [7] a rather special type of lower bound on generating functions for return probabilities of random walk on generic trees was proven. Here, we establish a natural generalization of that bound applicable to the cumulated probabilities $Q_G(n; v_0, v_0)$ associated with an arbitrary connected graph, as stated in the following theorem.

Theorem 1. *Let G be a connected graph and G_0 a finite connected sub-graph of G spanned by its set of vertices V_0 . Then*

$$Q_G(n; v_0, v_0) \geq \sigma_{v_0} \left(\frac{2|\overline{G_0}|}{n+1} + \mathcal{C}_{G, G_0}(n; v_0) \right)^{-1}, \tag{91}$$

for every vertex $v_0 \in G_0$, where $\mathcal{C}_{G,G_0}(n; v_0)$ is defined, up to a factor σ_{v_0} , as the probability for a walk starting at v_0 not to return to v_0 before leaving G_0 in at most n steps, that is

$$\mathcal{C}_{G,G_0}(n; v_0) = \sigma_{v_0} \sum_{v \in \partial_{in} G_0} \sum_{\substack{\omega : v_0 \rightarrow v \\ \omega \subseteq G_0, |\omega| \leq n}} p_G(\omega) \sigma_v^{-1} \sigma_v^{out}. \quad (92)$$

Proof. We define

$$\tilde{Q}_G(n; v, u) = \sigma_u^{-1} \sum_{\substack{\omega : v \rightarrow u \\ \omega \subseteq G_0, |\omega| \leq n}} p_G(\omega)$$

and note that $\tilde{Q}_G(n; v, u)$ vanishes if $v \notin V_0$ or $u \notin V_0$, while it satisfies the diffusion equation (78) for $v, u \in V_0$. Since the left-hand side of (78) is non-negative (as $\tilde{Q}(n; v, u)$ is a non-decreasing function of n), it follows from the maximum principle for the discrete Laplacian that $\tilde{Q}_G(n; v_0, u)$ assumes its maximal value as a function of u at $u = v_0$, i.e.

$$\tilde{Q}_G(n; v_0, u) \leq \tilde{Q}_G(n; v_0, v_0), \quad u \in G. \quad (93)$$

From (87) we have

$$n + 1 = \sum_{u \in G_0} \sigma_u \tilde{Q}_G(n; v_0, u) + \sum_{u \in G} \sum_{\substack{\omega : v_0 \rightarrow u \\ \omega \not\subseteq G_0, |\omega| \leq n}} p_G(\omega). \quad (94)$$

Using (93) and that

$$\sum_{u \in G_0} \sigma_u \leq 2 |\bar{G}_0|,$$

the first sum on the right-hand side in (87) can be estimated from above by

$$2 |\bar{G}_0| \tilde{Q}_G(n; v_0, v_0). \quad (95)$$

The last sum, on the other hand, can be estimated as follows. Any walk ω starting at v_0 which is not contained in G_0 can be decomposed in a unique way into a (possibly trivial) walk $\omega' : v_0 \rightarrow v_0$ which is contained in G_0 , followed by a walk $\omega'' : v_0 \rightarrow v$ which is likewise contained in G_0 but does not return to v_0 and such that $v \in \partial_{in} G_0$, and finally a step from v to a vertex $v' \in \partial_{out} G_0$ and a walk ω''' starting at v' . Obviously, the lengths of ω', ω'' and ω''' sum up to at most n and $p_G(\omega) = p_G(\omega') p_G(\omega'') \sigma_v^{-1} p_G(\omega''')$. Hence, an upper bound on the last term in (94) is obtained by relaxing the constraint $|\omega'| + |\omega''| + |\omega'''| = n$ to $|\omega'|, |\omega''), |\omega'''| \leq n$, in which case the sum factorizes into three terms: summation over ω' contributes a factor $\sigma_{v_0} \tilde{Q}_G(n; v_0, v_0)$, summation over ω'' is bounded by $n+1$ by (87), whereafter summation over ω'', v , and v' gives a factor $\sigma_{v_0}^{-1} \mathcal{C}_{G,G_0}(n; v_0)$. Hence, we have

$$\sum_{u \in G} \sum_{\substack{\omega: v_0 \rightarrow u \\ \omega \not\subseteq G_0, |\omega| \leq n}} p_G(\omega) \leq (n+1) \tilde{Q}_G(n; v_0, v_0) \mathcal{C}_{G, G_0}(n; v_0). \quad (96)$$

Using eqs. (94), (95), and (96) we finally arrive at

$$n+1 \leq \tilde{Q}_G(n; v_0, v_0) \left\{ 2|\overline{G}_0| + (n+1) \mathcal{C}_{G, G_0}(n; v_0) \right\},$$

which implies (91) since $\sigma_{v_0} \tilde{Q}_G(n; v_0, v_0) \leq Q_G(n; v_0)$.

Note that the relation of $\mathcal{C}_{G, G_0}(n; v_0)$ to an exit probability shows that it is bounded by σ_{v_0} . Clearly, $\mathcal{C}_{G, G_0}(n; v_0)$ is an increasing function of n so the limit

$$\mathcal{C}_{G, G_0}(v_0) = \lim_{n \rightarrow \infty} \mathcal{C}_{G, G_0}(n; v_0) = \sup_{n \geq 1} \mathcal{C}_{G, G_0}(n; v_0), \quad (97)$$

exists and is, by definition, the *effective conductance* of G between v_0 and the complement of G_0 . The *effective resistance* of G between v_0 and the complement of G_0 is defined as

$$\mathcal{R}_{G, G_0}(v_0) = (\mathcal{C}_{G, G_0}(v_0))^{-1}. \quad (98)$$

Clearly, (91) then implies

$$Q_G(n; v_0, v_0) \geq \sigma_{v_0} \left(\frac{2|\overline{G}_0|}{n+1} + \mathcal{R}_{G, G_0}(v_0)^{-1} \right)^{-1}, \quad (99)$$

Given graphs G and G_0 as above let us define \widehat{G}_0 to be the graph obtained from \overline{G}_0 by identifying all vertices in $\partial^{\text{out}} G_0$ with a single new vertex v_1 and leaving out all edges with both endpoints in $\partial^{\text{out}} G_0$.⁵ It is then clear that $\mathcal{C}_{G, G_0}(v_0) = \mathcal{C}_{\widehat{G}_0, \widehat{G}_0 - v_1}(v_0)$, which is called the conductance of \widehat{G}_0 between v_0 and v_1 . It will also be denoted by $\mathcal{C}_{\widehat{G}_0}(v_0, v_1)$. Since here \widehat{G}_0 can be any finite graph, this defines the conductance between any two different vertices v_0, v_1 in a finite connected graph H by

$$\mathcal{C}_H(v_0, v_1) = \sum_{\omega: v_0 \leftrightarrow v_1} \sigma_{v_0} p_H(\omega), \quad (100)$$

where we use the notation $\omega: v_0 \leftrightarrow v_1$ to denote a path from v_0 to v_1 that does not hit the end-vertices at intermediate steps. Clearly, $\mathcal{C}_H(v_0, v_1)$ is symmetric in v_0 and v_1 .

Recalling (82) and noting that any path $\omega: v_0 \rightarrow v_1$ can uniquely be decomposed into a path $\omega': v_0 \rightarrow v_0$ (possibly trivial) not hitting v_1 and a path $\omega'': v_0 \leftrightarrow v_1$ we get that

⁵ It should be noted that \widehat{G}_0 may contain multiple edges, but the reader may easily verify that all considerations in the present subsection apply with obvious modifications also to graphs with multiple edges.

$$\mathcal{C}_H(v_0, v_1) \sum_{\substack{\omega': v_0 \rightarrow v_1 \\ v_1 \notin \omega}} p(\omega') \sigma_{v_0}^{-1} = 1,$$

which implies that the resistance $\mathcal{R}_H(v_0, v_1) := (\mathcal{C}_H(v_0, v_1))^{-1}$ can be expressed as

$$\mathcal{R}_H(v_0, v_1) = \sum_{\substack{\omega: v_0 \rightarrow v_1 \\ v_1 \notin \omega}} p(\omega) \sigma_{v_0}^{-1}. \quad (101)$$

The relation of these definitions to the physical notion of conductance and resistance in electrical networks is perhaps not obvious at this stage. From (100) it is clear that conductance and resistance of a single edge are equal to 1 and it is simple to verify, using (100) and (101), that the standard laws for composing resistances in a series or in parallel hold. We refer to Ch. 2 of [17] for a more general and detailed account of these aspects, including Rayleigh's Monotonicity Principle which states that the effective resistance is a non-decreasing function of the edge-resistances. In our case of unit edge resistances this principle implies that contracting an edge in H that does not connect v_0 and v_1 , i.e. deleting the edge and identifying its end-vertices, reduces the resistance $\mathcal{R}_H(v_0, v_1)$ or leaves it unchanged.

We remark that the inequality (84) can now be rewritten as

$$\mathcal{R}_H(v_0, v_1) \leq d_H(v_0, v_1) \quad (102)$$

for any pair of different vertices v_0, v_1 in a finite connected graph H . Moreover, we have that equality holds if H is a tree, i.e.

$$\mathcal{R}_T(v_0, v_1) = d_T(v_0, v_1) \quad \text{if } T \text{ is a finite tree.} \quad (103)$$

Indeed, if $d_T(v_0, v_1) = 1$ only one path consisting of the edge connecting v_0 and v_1 contributes on the right-hand side of (100) and gives 1. If $d_T(v_0, v_1) = k \geq 2$, let v be a vertex in the interior of the unique path connecting v_0 and v_1 and let T_1 be the sub-tree of T spanned by v and its descendants when considering v_0 as the root of T , and let T_0 be the tree spanned by the remaining vertices and v . Then T_0 and T_1 only share the single vertex v and hence by the law of coupling resistances in a series we have

$$\mathcal{R}_T(v_0, v_1) = \mathcal{R}_{T_0}(v_0, v) + \mathcal{R}_{T_1}(v, v_1).$$

The claim (103) now follows trivially by induction.

Given a rooted graph G , let $\mathcal{R}(R)$ denote the resistance between the root v_0 and the complement of the ball $B_R(G)$ of radius R around the root, and assume that for some $\kappa \geq 0$ it holds for R large that

$$\mathcal{R}(r) \geq \text{const. } R^\kappa.$$

Note that (102) implies the constraint

$$\kappa \leq 1. \quad (104)$$

If the Hausdorff dimension d_h of G exists we obtain, by choosing $G_0 = B_R(G)$ in (91) where $R = \lfloor n^{\frac{1}{d_h + \kappa}} \rfloor$, that

$$Q_G(n; v_0, v_0) \geq \text{const. } n^{\frac{\kappa}{d_h + \kappa}}$$

and hence,

$$d_s \leq \frac{2d_h}{d_h + \kappa}, \quad (105)$$

thus supplementing the lower bound (81).

If G_0^K , $K = 1, 2, 3, \dots$, is a sequence of finite connected graphs as in Theorem 1 containing a fixed vertex v_0 and such that the graph distance from v_0 to $\partial_{in} G_0^K$ tends to infinity as $K \rightarrow \infty$, then $\sigma_{v_0}^{-1} \lim_{K \rightarrow \infty} \mathcal{C}_{G, G_0^K}(v_0)$ exists and equals the escape probability from v_0 , that is the probability for an infinite walk starting at v_0 never to return to v_0 . Hence, by the discussion of recurrency in Section 7.1, we conclude that this quantity vanishes exactly if G is recurrent. In particular, we get that if G is recurrent then $\mathcal{C}_{G, G_0^K}(n; v_0)$ converges to 0 uniformly in n as $K \rightarrow \infty$. In order to exploit Theorem 1 we need more detailed information on the decay rate of $\mathcal{C}_{G, G_0^K}(n; v_0)$ or $\mathcal{C}_{G, G_0^K}(v_0)$ for an appropriate choice of G_0^K . This is a non-trivial problem for general graphs, but if G is a tree we can make use of (103) as will be seen.

We are now in a position to apply the previous results to the case of generic random trees and prove the desired upper bound on their spectral dimension. Recalling the one-spine character of the generic trees we let T be such a tree and aim at applying Theorem 1 with G_0^K equal to the sub-tree spanned by the vertices of the (finite) branches rooted at the spine vertices s_1, \dots, s_K .

Denoting as previously by Br_i the union of the branches rooted at a fixed spine vertex s_i , we then have

$$|\overline{G}_0^K| = \sum_{i=1}^K |Br_i| + K + 1, \quad (106)$$

and obviously, $|\overline{G}_0^K| \geq |B_K|$. We can now use (21) to estimate the growth rate of $|G_0^K|$ by first establishing the following lemma.

Lemma 1. *There exist constants $\bar{c} > 0$ and $u_0 > 0$ such that for all $K \geq 1$ and all $u > u_0$ the following inequality holds:*

$$\nu \left(\{T : K^{-2} |\overline{G}_0^K| \geq u\} \right) \leq \frac{\bar{c}}{\sqrt{u}}. \quad (107)$$

Proof. By (106) it clearly suffices to show (107) with $X_K = \sum_{i=1}^K |Br_i|$ replacing $|\overline{G}_0^K|$. We take as starting point the following inequality which can be found, e.g., in [22, Section 8.7]:

$$\nu(\{X_K \geq u\}) \leq \alpha u \int_0^{\frac{1}{u}} \left(1 - \text{Re } \overline{Z}(e^{iv})^K\right) dv, \quad (108)$$

where α is a universal constant and $\bar{Z}(e^{iv})^K$ is the characteristic function of X_K as a sum of K independent and identically distributed (i.i.d.) random variables. From (21) we have

$$\bar{Z}(e^{iv}) = e^{\bar{c}_0 \sqrt{1-e^{iv}} + O(|1-e^{iv}|)}$$

and hence, for $v > 0$ sufficiently small,

$$\begin{aligned} \operatorname{Re} \bar{Z}(e^{iv})^K &= \operatorname{Re} e^{K \bar{c}_0 \sqrt{1-e^{iv}} + KO(|1-e^{iv}|)} \\ &= \operatorname{Re} e^{K \bar{c}_0 \sqrt{-iv+O(v^2)} + KO(v)} \\ &= \operatorname{Re} e^{\frac{1}{\sqrt{2}} \bar{c}_0 K (1-i) \sqrt{v} \sqrt{1+O(v)} + KO(v)} \\ &= e^{\frac{1}{\sqrt{2}} \bar{c}_0 K \sqrt{v} + KO(v)} \cos \left(\frac{1}{\sqrt{2}} \bar{c}_0 K \sqrt{v} + KO(v) \right). \end{aligned}$$

By Taylor expanding the exponential and cosine functions it follows that there exists a $\delta > 0$ such that

$$1 - \operatorname{Re} \bar{Z}(e^{iv})^K = \frac{1}{\sqrt{2}} \bar{c}_0 K \sqrt{v} + O(K^2 v) \leq \bar{c}_0 K \sqrt{v}, \quad \text{for } 0 \leq K \sqrt{v} \leq \delta.$$

Using this estimate in (108) we get

$$\nu(\{X_K \geq u\}) \leq \frac{2\alpha \bar{c}_0 K}{3\sqrt{u}}$$

if $\frac{K}{\sqrt{u}} \leq \delta$. Upon replacing u by uK^2 the claimed inequality follows for $u \geq \delta^{-2}$ with $\bar{c} = \frac{2}{3}\alpha \bar{c}_0$.

Setting $K = 2^M$ and $u = M^3$ in (107) we get

$$\sum_{M=1}^{\infty} \nu \left(\{T : 4^{-M} |\bar{G}_0|^{2^M} \geq M^3\} \right) < \infty.$$

Hence, by the Borel-Cantelli lemma, we conclude that with probability 1 it holds that

$$|\bar{G}_0|^{2^M} \leq M^3 4^M \quad (109)$$

for $M > M_0$ where M_0 is an integer depending on T . Furthermore, given an arbitrary $K \geq 1$, we can choose M such that $2^{M-1} \leq K \leq 2^M$ and conclude that

$$|\bar{G}_0^K| \leq |\bar{G}_0|^{2^M} \leq M^3 4^M \leq 4K^2 \left(\frac{\ln K}{\ln 2} + 1 \right)^3 \leq c_1 K^2 (\ln K)^3 \quad (110)$$

for $K > K_0$, where $c_1 > 0$ is a numerical constant independent of T while K_0 may depend on T .

For a fixed $T \in \mathcal{T}_\infty$ as above let $n \geq 1$ be given and let $K = \lfloor n^{\frac{1}{3}} \rfloor$ and assume n is large enough so that $K > K_0$. It then follows from (91) and (110) that

$$Q_T(n; s_0, s_0) \geq Q_T(K^3; s_0, s_0) \geq \left(\frac{c_1 K^2 (\ln K)^3}{K^3 + 1} + K^{-1} \right)^{-1} \geq C_1 (\ln n)^{-3} n^{\frac{1}{3}}, \quad (111)$$

where $C_1 > 0$ is a constant and we have also used that $\mathcal{C}_{T, G_0^K}(s_0) = (K + 1)^{-1}$ by (103). Using (80), the definition of d_s , it follows that $d_s \leq \frac{4}{3}$ with probability 1.

For the sake of completeness we mention that by elaborating on the upper bound (89) on $Q_T(n; s_0, s_0)$ in a similar way as above and using the lower bound on $|B_R(T)|$ in (72), we obtain an upper bound on $Q_T(n; s_0, s_0)$ analogous to (111). More precisely, one gets that

$$C_1 (\ln n)^{-3} n^{\frac{1}{3}} \leq Q_T(n; s_0, s_0) \leq C_2 (\ln n)^2 n^{\frac{1}{3}}$$

for a suitable constant $C_2 > 0$, which of course also implies $d_s = \frac{4}{3}$.

7.4 Spectral dimension of causal triangulations

In this section we show that the spectral dimension of the CDT ensemble defined in Section 4 equals 2. Thus, even though the Hausdorff dimensions of the CDTs and of the corresponding generic tree are identical the spectral dimensions are not. This is due to the higher connectivity of the CT which leads to different behaviour of the resistance between the root and the complement of the ball around the root for large radius.

To obtain the upper bound $d_s \leq 2$ we make use of an argument that is most easily understood in terms of resistance estimates. Considering an arbitrary infinite causal triangulation G , let G_R be the graph obtained from the ball $B_R(G)$ by collapsing its boundary to a single vertex u (i.e. by contracting all the boundary edges). Then the resistance of G between the central vertex S_0 and the complement of the ball $B_R(G)$ is identical to the resistance of G_R between S_0 and u . By contracting the edges in each S_r , $r = 1, \dots, R$, we obtain, by the Rayleigh Monotonicity Principle, a network with lower resistance between S_0 and u . On the other hand, this network is a series of resistances $\mathcal{R}_0, \mathcal{R}_1, \dots, \mathcal{R}_R$, where \mathcal{R}_k is the resistance of $\Delta(\Sigma_k)$ unit resistances connected in parallel. Hence,

$$\mathcal{R}_{G, B_R}(S_0) \geq \sum_{k=0}^R \frac{1}{\Delta(\Sigma_k)}. \quad (112)$$

In order to make use of (99) we need a suitable lower bound on the resistance $\mathcal{R}_{G, B_R}(S_0)$. In view of (112) we therefore want to estimate the probability $\rho(\{G : \Delta(\Sigma_k) > K\})$. For this purpose we use (16) to write

$$\rho(\{G : B_R(G) = B_R(G_0)\}) = D_R(G_0) 2^{D_R(G_0)+1} 2^{-\|B_R(G_0)\|} \quad (113)$$

for any fixed infinite causal triangulation $G_0 \in \mathcal{C}$, where it is used that $Z_0 = \frac{1}{2}$ and $\zeta_0 = \frac{1}{4}$ in (16) for the uniform planar tree and also $\|B_R(G_0)\| = |B_{R+1}(\beta(G_0))|$. Since the number of causal triangulations of the annulus Σ_k with l_k vertices on the inner boundary, among which one is marked, and l_{k+1} vertices on the outer boundary equals $\binom{l_k + l_{k+1} - 1}{l_k - 1}$, it follows by a straight-forward combinatorial argument that

$$\rho(\{G : D_R = l_R, D_{R+1} = l_{R+1}\}) = l_{R+1} 2^{-l_{R+1}} \binom{l_R + l_{R+1} - 1}{l_R - 1} \frac{1}{R(R-1)} \left(\frac{R-1}{2R}\right)^{l_R}, \quad (114)$$

see [16] for details. Summing this identity over $l_R + l_{R+1} > K$ then yields

$$\rho(\{G : \Delta(\Sigma_R) > K\}) = \frac{K + 2R - 1}{2R - 1} \left(1 - \frac{1}{2R}\right)^K. \quad (115)$$

Now, let $a > 2$ be fixed and define

$$\mathcal{A}_R = \{G : \Delta(\Sigma_R) > aR \ln R\}.$$

Then (115) implies that $\rho(\mathcal{A}_R) \leq (1 + a \ln R) R^{-a}$, and hence

$$\sum_{R=1}^{\infty} \rho(\mathcal{A}_R) < \infty.$$

By the Borel-Cantelli lemma it follows that with probability 1 it holds that

$$\Delta(\Sigma_R) \leq aR \ln R$$

for R large enough. Consequently, for all such $G \in C_{\infty}$ we have

$$\mathcal{R}_{G, B_R}(S_0) \leq \text{const.} \sum_{k=1}^R (ak \ln k)^{-1} \leq \text{const.} \ln \ln R. \quad (116)$$

Setting $R = \lfloor n^{\frac{1}{3}} \rfloor$ in (99) it follows from the bound (110) and the previous estimate that

$$Q_G(n; S_0, S_0) \geq \left(\frac{c_1 R^2 (\ln R)^3}{n+1} + (a \ln \ln R)^{-1} \right)^{-1} \geq C'_1 \ln \ln n \quad (117)$$

for a suitable constant $C'_1 > 0$ (depending on G). By the definition of d_s this evidently implies the desired upper bound $d_s \leq 2$.

To obtain a useful upper bound on $Q_G(n; S_0, S_0)$ the inequality (89) is not applicable since it does not capture the dependence of d_s on the behaviour of the resistance between the root and the complement of balls at large radii. In our particular case, however, the bound

$$Q_G(n; S_0) \leq \sigma_{S_0} \mathcal{R}_{G, B_R}(S_0) \quad \text{for } n \leq R, \quad (118)$$

which follows immediately from the definitions of Q_G and $\mathcal{R}_{G, B_R}(S_0)$, is sufficient, provided a suitable upper bound on the resistance can be obtained. In [23] it is shown by an argument requiring rather advanced probabilistic techniques that the bound

$$\mathcal{R}_{G, B_R}(S_0) \leq e^{\text{const.} \sqrt{\ln R}}$$

holds for R sufficiently large with probability 1. Hence, it follows by setting $R = n^b$ in (118), where $b \geq 1$, that with probability 1 we have

$$Q_G(n; S_0) \leq \sigma_{S_0} e^{\text{const.} \sqrt{\ln n}}$$

for n large enough. Clearly, this implies the lower bound $d_s \geq 2$.

8 Curvature and matter fields on the CDT

Modifications of the graph weights, by introducing terms that bias the vertex degree, or adding extra degrees of freedom (often referred to as ‘matter fields’) to the graphs, might lead to different critical behaviour. Some of these modifications can be analysed using the bijection β , but understanding of others remains seriously incomplete. Some examples are discussed here in the grand canonical ensemble framework.

8.1 Curvature

The simplest elaboration of the graph weights is to introduce an extra factor $q^{\sigma_v - 6}$ for each vertex into the definition of W_M (49). This is the analogue of including the Ricci scalar curvature term from the Einstein action in a continuum gravity theory. It is trivial at fixed topology in two dimensions because $\sum_{v \in G} (\sigma_v - 6)$ is proportional to the Euler characteristic of G so W_M is simply multiplied by a constant.

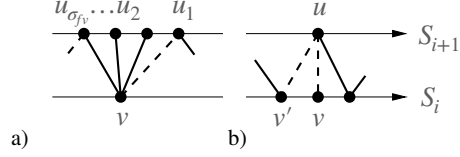
A different higher curvature term was proposed by [12]. Recalling the definition of σ_{bv} and σ_{fv} from Section 4.1, introduce the extra factor

$$Q(p, q) = \prod_{v \in G \setminus S_0} q^{\frac{1}{2}|\sigma_{fv} - 2|} p^{\frac{1}{2}|\sigma_{bv} - 2|} \quad (119)$$

into the graph weight for the disk partition function (49). Decreasing q, p from 1 enhances the weight for vertices which belong to 3 triangles each in the forward and backward direction and thus introduces a bias towards graphs that, at least locally, are regular triangulations of the plane. (It was argued in [24] that this is equivalent to the naive discretization of an extrinsic curvature squared term in the continuum

gravity action.) However, it is straightforward to see that the critical properties of W_M [16] remain unchanged as follows. Consider a vertex $v \in S_i(G)$ which shares

Fig. 7 The neighbourhood of a vertex $v \in G$ when a) $\sigma_{fv} > 1$, and b) $\sigma_{fv} = 1$. Dashed lines represent edges that are present in G but not in the tree $T = \beta(G)$.



edges with $u_m \in S_{i+1}(G)$, $m = 1, \dots, \sigma_{fv}$, see Fig. 7 a. Then, making use of the bijection β , the q -dependent part of (119) is given by,

$$\prod_{v \in G} q^{\frac{1}{2}|\sigma_{fv}-2|} = \prod_{v \in \beta(G): \sigma_{fv} \geq 2} q^{\frac{1}{2}(\sigma_{fv}-2)} \prod_{u \in \beta(G): \sigma_{fu}=1} q^{\frac{1}{2}}. \quad (120)$$

The p -dependent part of (119) can be rewritten to give

$$\prod_{v \in G \setminus S_0} p^{\frac{1}{2}|\sigma_{bv}-2|} = \prod_{v \in G \setminus S_0: \sigma_{bv} > 1} p^{\frac{1}{2}(\sigma_{bv}-2)} \prod_{u \in G \setminus S_0: \sigma_{bu}=1} p^{\frac{1}{2}}. \quad (121)$$

Vertices $u \in G$ with $\sigma_{bu} = 1$ cannot be the leftmost descendant of a vertex $v \in \beta(G)$, see Fig. 7 a. So each vertex $v \in \beta(G)$ with $\sigma_{fv} \geq 2$ is associated with precisely $\sigma_{fv} - 2$ vertices $u \in G$ with $\sigma_{bu} = 1$ which gives

$$\prod_{u \in G \setminus S_0: \sigma_{bu}=1} p^{\frac{1}{2}} = \prod_{u \in \beta(G): \sigma_{fu} \geq 2} p^{\frac{1}{2}(\sigma_{fu}-2)}. \quad (122)$$

Finally, vertices $u \in S_{i+1}(G)$ with $\sigma_{bu} > 1$ must be the leftmost descendant of a vertex $v \in \beta(G)$, see Fig. 7 b; each vertex $v' \in S_i(G)$ with $\sigma_{fv'} = 1$ then increments σ_{bu} by one, so,

$$\prod_{v \in G \setminus S_0: \sigma_{bv} > 1} p^{\frac{1}{2}(\sigma_{bv}-2)} = \prod_{u \in \beta(G): \sigma_{fu}=1} p^{\frac{1}{2}}. \quad (123)$$

Combining (119)-(123) gives

$$\mathcal{Q}(p, q) = \prod_{v \in \beta(G): \sigma_{fv} \geq 2} (pq)^{\frac{1}{2}(\sigma_{fv}-2)} \prod_{u \in \beta(G): \sigma_{fu}=1} (pq)^{\frac{1}{2}}, \quad (124)$$

so that each leaf in $T = \beta(G)$ gets a weight $(pq)^{\frac{1}{2}}$, and all other vertices a weight $(pq)^{\frac{1}{2}(k_v-1)}$, where k_v is the number of descendants.

Without loss of generality set $p = q$; the recurrence (55) is then replaced by

$$\begin{aligned}\tilde{w}_h(g, q, z) &= q + \sum_{k=1}^{\infty} g^{2k} q^{k-1} (\tilde{w}_{h-1}(g, q, z))^k \\ &= \frac{q + g^2(1 - q^2)\tilde{w}_{h-1}(g, q, z)}{1 - g^2 q \tilde{w}_{h-1}(g, q, z)}.\end{aligned}\quad (125)$$

It is easy to show (by direct substitution in (125), and using (55)) that the solution satisfying $\tilde{w}_1(g, q, z) = zg^{-1}$ is

$$\tilde{w}_h(g, z) = q - q^{-1} + \frac{q^{-1}}{1 + g^2(1 - q^2)} w_h\left(\frac{g}{1 + g^2(1 - q^2)}, qz + g(1 - q^2)\right). \quad (126)$$

It follows from (59) that the functions $\tilde{w}_h(g, z)$ for every h are analytic in the region

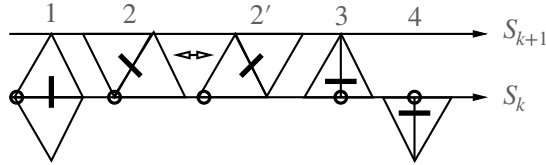
$$A : |g| < (1 + q)^{-1}, \quad |z| < 1, \quad (127)$$

so this modification has no effect on the large graph behaviour and the model is in the same universality class for all q . It is clearly possible to define curvature dependent weights that take a form different from (119), for example $q^{|\sigma_{fv} + \sigma_{bv} - 4|}$ or $q^{(\sigma_{fv} + \sigma_{bv} - 4)^2}$; but nothing is known about such systems.

8.2 Dimers

Dimer models on fixed lattices exhibit a rich structure. In particular they have a critical point, at which the dimers condense, whose scaling limit is related to the Lee-Yang singularity and is described by a conformal field theory (CFT) [25]. The model of dimers coupled to CTs, defined below, can be solved by a bijection, which is a generalization of β , to labelled trees [26, 27, 28, 29]. There are new phases in which the interaction between the dimers and the graphs becomes strong and changes the universality class from the pure CT case of Section 5.1. The steps to demonstrate this are outlined here, full details are in [29].

Fig. 8 The possible types of dimer on a CT, together with their index; the vertex that owns the dimer in each case is marked with a circle. The double arrow indicates the equivalence of types 2 and 2' in W_M .



Dimers are objects that are dual to edges, and may be assigned freely subject to the *dimer rule* that each triangle is allowed to contain only one dimer. The possible types of dimer on a CT, and the vertices which ‘own’ them, are shown in Fig. 8; we will assume that there are no dimers allowed on the edges that are attached to the

central vertex S_0 , or that enter the boundary triangles of $G \in C^{(h)}$. We denote the dimer configurations allowed by the dimer rule for $G \in C$ by $\mathcal{L}(G)$; and the number of times a dimer of type i appears in a dimer configuration $l \in \mathcal{L}(G)$ by l_i . The disk partition function for this model is then defined by assigning each dimer of type i a weight ξ_i and is given by

$$W_M(g, \{\xi\}, z; h) = \sum_{G \in C^{(h)}} \sum_{l \in \mathcal{L}(G)} |S_{h-1}(G)| (z/g)^{|S_{h-1}(G)|} g^{\Delta(G)} \xi_1^{l_1} \xi_2^{l_2} \xi_{2'}^{l_{2'}} \xi_3^{l_3} \xi_4^{l_4}. \quad (128)$$

A crucial simplification [26] is provided by the observation that, for every graph-and-dimer configuration with a type $2'$ dimer there is another which differs only by having a type 2 dimer on a flipped edge, see Fig 8. It follows that

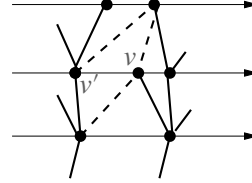
$$W_M(g, \xi_1, \xi_2, \xi_{2'}, \xi_3, \xi_4, z; h) = W_M(g, \xi_1, \xi_2 + \xi_{2'}, 0, \xi_3, \xi_4, z; h), \quad (129)$$

so $\xi_{2'}$ can be set to zero, and the sum over dimer configurations limited to those with no type $2'$ dimers. It is convenient also to let type 0 mean no dimer and then define $\xi = \{\xi_0 = 1, \xi_1, \xi_2, \xi_3, \xi_4\}$. We see, by applying the dimer rule, that each vertex v can own at most one of the type 0, 1, 2, 3 dimers, and that if it owns a type 0, 2, 3 dimer it can also own a type 4, but that the combination of type 1 and type 4 is forbidden. So we assign to v a two-component label ℓ_v , denoting the dimers it owns, which can take values

$$\ell_v = (p_v, q_v) \in \{0, 1, 2, 3\} \times \{0, 4\} \setminus \{(1, 4)\}. \quad (130)$$

The dimer rule then implies a set of constraints \mathcal{N} on the allowed labels, ℓ_v and $\ell_{v'}$, of neighbouring vertices, v and v' , in $G \in C$.

Fig. 9 Dashed lines represent edges that are present in G but not in the tree $T = \beta(G)$. If $p_{v'} = 3$ then $p_v = 1$ is forbidden, which is a non-local constraint on T .



Since each $v \in G$ is also a vertex of the corresponding tree $T = \beta(G)$ the labels ℓ_v can also be associated with the vertices of T . Then \mathcal{N} induces a set of rules for the labelling of $v \in T$ [29]. These rules are local in T with one exception which is illustrated in Fig.9. Two vertices which are nearest neighbours in G can be arbitrarily widely separated in T ; we deal with this non-local constraint in T by forbidding $p_v = 3$ if v is the most anticlockwise descendant of another vertex. The outcome is a model of dimers on CT that is equivalent to a model of labelled trees with a set of local constraints $\tilde{\mathcal{N}}$ on the labels; this model can in turn be solved by generalizing the methods of Section 5.

To solve this model by the decomposition used in Section 5, we have to keep track of the label ℓ assigned to the vertex adjacent to the root of the tree T (the root itself has no label). We then denote the allowed label configurations by $\mathcal{L}^\ell(T)$ and define the corresponding partition function

$$w_h^\ell(g, \xi, z) = \sum_{h' \leq h} \sum_{T \in \mathcal{T}^{(h')}} \sum_{l \in \mathcal{L}^\ell(T)} (z/g)^{|S_h(T)|} \left(\prod_{v \in T \setminus r} g^{2(\sigma_v - 1)} \xi_{p_v} \xi_{q_v} \right). \quad (131)$$

It is easy to show, by the arguments used in Section 5.1, that the disk partition function is given by

$$W_M(g, \xi, z; h) = g^2 z \frac{\partial}{\partial z} w_h^{(0,0)}(g, \xi, z). \quad (132)$$

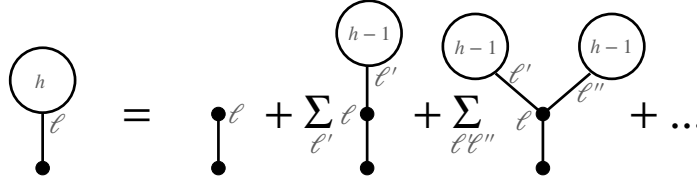


Fig. 10 The decomposition of trees leading to (133). The sums over labels are constrained to satisfy the labelling rules \mathcal{N} .

The trees contributing at height h to (131) can be decomposed into trees of height $h-1$ as shown in Fig. 10. The local nature of the labelling rules ensures that it is only necessary to keep track of the labels at the first vertex of the component trees so the right hand side is still made up of geometric series, albeit more complicated than for the case without dimers (55). The relationships obtained by resumming these series can be reduced to just two for $w_h^{(0,0)}$ and $w_h^{(2,0)}$ which take the form

$$w_{h+1}^{(0,0)} = F^{(1)}(w_h^{(0,0)}, w_h^{(2,0)}, g, \xi), \quad w_{h+1}^{(2,0)} = F^{(2)}(w_h^{(0,0)}, w_h^{(2,0)}, g, \xi), \quad (133)$$

where

$$\begin{aligned} F^{(1)}(f_1, f_2, g, \xi) &= \frac{1}{1 - B}, \\ F^{(2)}(f_1, f_2, g, \xi) &= \frac{\xi_2}{1 - B} \left(\frac{g^2 f_1 + g^2 f_2 + g^4 \xi_3 f_1}{1 - g^4 \xi_3 \xi_4 f_1} \right), \\ B &= g^2 \xi_1 f_1 + g^4 \xi_4 \xi_3 f_1 + \frac{g^2 (g^2 \xi_3 f_1 + f_1 + f_2) (1 + g^2 \xi_4 f_1 + g^2 \xi_4 f_2)}{1 - g^4 \xi_3 \xi_4 f_1}. \end{aligned} \quad (134)$$

Iterating these relations with initial data $w_1^\ell(g, \xi, z)$ (which are easily computed) will give the partition functions for any finite height h .

The grand canonical partition functions unconstrained by height are given by

$$w_\infty^\ell(g, \xi) = \sum_{T \in \mathcal{T}} \sum_{l \in \mathcal{L}^\ell(T)} \left(\prod_{v \in T \setminus r} g^{2(\sigma_v - 1)} \xi_{p_v} \xi_{q_v} \right). \quad (135)$$

They are simply the fixed points of the recurrence equations so satisfy (133) with $w_{h+1}^\ell = w_h^\ell = w_\infty^\ell$ for $\ell = (0, 0), (2, 0)$. These equations reduce to a quartic equation for $w_\infty^{(0,0)}$ which can in principle be solved exactly to determine the partition functions, although the explicit form of the solutions is not very useful and we will proceed in a different way. The solutions are also the limits, if these exist, of the sequences $\mathcal{S}^\ell = (w_h^\ell, h = 1, 2, \dots)$.

As usual we expect that the functions $w_h^\ell(g, \xi, z)$ for every h , and the function $w_h^\infty(g, \xi)$, are analytic in some region

$$A_\xi : |g| < g_c(\xi), |z| < z_c(\xi). \quad (136)$$

However this depends upon the sequences \mathcal{S}_ℓ being smooth and converging to w_∞^ℓ . If $\xi_i \geq 0, \forall i$ then $F^{(1)}, F^{(2)}$ are positive convex functions of their first two arguments and the properties of the system are basically the same as for the pure CT model; the presence of the dimers does not drive any change in the geometrical properties, and there is no long-range cooperative behaviour of the dimers themselves. If the ξ_i are sufficiently negative then convexity is no longer guaranteed so this behaviour can change. Indeed if they are too negative then the sequences \mathcal{S}^ℓ become oscillatory, and the model has no meaning in the statistical mechanical sense. New and interesting physics emerges for an intermediate set of dimer weights Ξ which separate the CT-like region from the oscillatory region.

We proceed by analysing the behaviour in the vicinity of $g = g_c(\xi)$ assuming the convergence properties discussed above. Adopting the simplified notation $w_\infty^1 \equiv w_\infty^{(0,0)}(g, \xi)$ and $w_\infty^2 \equiv w_\infty^{(2,0)}(g, \xi)$ we have

$$w_\infty^k = F^{(k)}(w_\infty^1, w_\infty^2, g, \xi), \quad k = 1, 2, \quad (137)$$

and

$$\frac{\partial w_\infty^k}{\partial g} = \left((1 - \mathbb{T})^{-1} \right)^{kl} \frac{\partial}{\partial g} F^{(l)}(w_\infty^1, w_\infty^2, g, \xi), \quad (138)$$

where

$$\mathbb{T}^{kl} = \frac{\partial}{\partial w_\infty^l} F^{(k)}(w_\infty^1, w_\infty^2, g, \xi) \equiv F_l^{(k)}. \quad (139)$$

At $g = 0$, \mathbb{T} vanishes; as $g \uparrow g_c(\xi)$, w_∞^k develops non-analytic behaviour when the largest eigenvalue of \mathbb{T} reaches one. We will denote: by w_c^k the value of w_∞^k at $g_c(\xi)$;

by $(\lambda_1 = 1, \lambda_2)$ the eigenvalues at criticality of $\mathbb{T} = \mathbb{T}_c$; by $u_{1,2}$ the corresponding eigenvectors; and by $\bar{u}_{1,2}$ vectors orthogonal to $u_{1,2}$ respectively. \mathbb{T}_c is not symmetric and it can be shown that, if the second eigenvalue $\lambda_2 = 1$, then for some values of ξ it has Jordan normal form where u_1 is a regular eigenvector and $\mathbb{T}_c u_2 = u_2 + \epsilon(\xi)u_1$.

Expanding (137) about the critical point by setting

$$\begin{aligned} w_\infty^i &= w_c^i + \phi^i, \\ g &= g_c(\xi) - \Delta g, \end{aligned} \quad (140)$$

we obtain

$$\begin{aligned} (1 - \mathbb{T})^{ij} \phi^j &= -\Delta g \left(\frac{\partial F^{(i)}}{\partial g} + \frac{\partial \mathbb{T}^{ij}}{\partial g} \phi^j \right) + \frac{1}{2} F_{lk}^{(i)} \phi^l \phi^k \\ &+ \frac{1}{3!} F_{klm}^{(i)} \phi^k \phi^l \phi^m + O((\Delta g)^2, \phi^4). \end{aligned} \quad (141)$$

The different phases of the model arise when ξ is tuned so that particular combinations of the coefficients in (141) vanish. With no constraints on these coefficients we obtain the generic case whose behaviour is the same as the pure CT model,

$$\phi^i = -\phi_c(\xi)(\Delta g)^{\frac{1}{2}} u_1^i + O(\Delta g), \quad (142)$$

where $\phi_c(\xi) > 0$. Imposing the constraint

$$\bar{u}_2^i (u_1^l F_{lk}^{(i)} u_1^k) = 0, \quad (143)$$

leads to the *Tri-critical* phase in which

$$\phi^i = -\phi_c(\xi)(\Delta g)^{\frac{1}{3}} u_1^i + O((\Delta g)^{\frac{2}{3}}). \quad (144)$$

Imposing the additional constraint

$$\bar{u}_{2c}^i \frac{\partial F^{(i)}}{\partial g} = 0, \quad (145)$$

leads to the *Dense Dimer* phase. In this case ϕ_i behaves as in (142) but other properties are different as we discuss next. The constraints (143) and (145) are conditions on the dimer weights ξ ; the first defines the region Ξ introduced above.

The unconstrained disk partition functions (135) can be written in the form

$$w_\infty^\ell(g, \xi) = \sum_{N=1}^{\infty} w_N^\ell(\xi) g^{2N}. \quad (146)$$

It follows by general considerations from (142) and (144) that

$$\lim_{N \rightarrow \infty} \frac{\log w_N^\ell(\xi)}{N} = -\log g_c(\xi); \quad (147)$$

therefore $\mu(\xi) = -\log g_c(\xi)$ is the thermodynamic free energy density, and the dimer density is then defined by $\chi(\xi) = -\xi_j \partial_{\xi_j} \log g_c(\xi)$. In the pure CT phase $\chi(\xi)$ is an analytic function, but as ξ approaches $\xi_c \in \Xi$ it develops non-analytic behaviour,

$$\chi(\xi) = R_1(\xi) + R_2(\xi)|\xi - \xi_c|^\sigma, \quad (148)$$

where $R_{1,2}$ are regular functions and σ is usually called the dimer (density) exponent. If ξ_c is in the Tri-critical phase, $\sigma = \frac{1}{2}$ and χ itself remains finite but its derivative diverges; on the other hand if ξ_c is in the Dense Dimer phase then $\sigma = -\frac{1}{3}$, χ diverges at $\xi = \xi_c$ and the dimers condense, hence the name.

For each of the new phases, the local Hausdorff dimension d_h and the scaling amplitude can be calculated. Although these phases only occur when dimer weights are negative, and individual graph weights can certainly be negative, it turns out that the theory at $g = g_c$ is nonetheless described by a bijection to a labelled single spine tree [28]. Thus, formally, at the level of expectation values it is possible to repeat the considerations of Section 6; when $\lambda_2 < 1$ we find that $d_h = 1$, which is not very interesting from the physical point of view. However there is still some freedom in the choice of ξ which can be adjusted to impose the condition that \mathbb{T}_c is not diagonalizable but has a Jordan normal form; this causes the finite trees attached to the spine in a typical graph to become more bushy, and for both the Tri-critical and Dense Dimer phases it can be shown that

$$\langle B_R \rangle = \text{const. } R^3 + O(R^2), \quad (149)$$

so the local Hausdorff dimension $d_h = 3$. Unlike the pure CT case of Section 5.1, the disk partition functions at finite h cannot be computed in closed form but their structure is very similar. Formally the scaling amplitudes are defined by setting $g = g_c(\xi) - \theta^{d_H}$, $y = y_c(\xi)(1 - Y\theta\Lambda^{-d_H^{-1}})$, $h = H\theta^{-1}\Lambda^{-d_H^{-1}}$ and taking $\theta \rightarrow 0$,

$$W_M^s(\Lambda, \xi, Y; H) = \lim_{\theta \rightarrow 0} W_M(g_c(\xi) - \theta^{d_H}, y_c(\xi)(1 - Y\theta\Lambda^{-d_H^{-1}}), H\theta^{-1}\Lambda^{-d_H^{-1}}). \quad (150)$$

In practice they can be computed in the scaling limit where the finite difference equations (133) become solvable differential equations. In the Tri-critical phase, $d_H = 3$ and

$$W_M^s(\Lambda, Y, H) = \text{const.} \frac{\sum_i \alpha_i e^{-\alpha_i \Lambda^{\frac{1}{3}} H}}{\left(\sum_i (\alpha_i^2 \Lambda^{\frac{1}{3}} + \alpha_i Y) e^{\alpha_i \Lambda^{\frac{1}{3}} H} \right)^2}, \quad (151)$$

where the sum runs over the three cube roots of unity, α_i , $i = 1, 2, 3$. While this amplitude has an exponential decay envelope similar to the CT case (61), it has os-

cillations superimposed. This reflects the negative dimer weights; taking the weights more negative destroys the convergence of the sequences \mathcal{S}^ℓ so the scaling limit no longer exists. In the Dense Dimer phase, $d_H = 2$ and

$$W_M^s(\Lambda, Y, H) = \text{const.} \frac{\Lambda}{\left(\Lambda^{\frac{1}{2}} \sinh H\Lambda^{\frac{1}{2}} + Y \cosh H\Lambda^{\frac{1}{2}}\right)^2}. \quad (152)$$

From the physical point of view this is the most interesting phase. At large H the behaviour of W_M^s deviates from the pure CT case by exponentially damped terms, as if there is some kind of matter interacting weakly with gravity. This is consistent with what is known numerically about other matter degrees of freedom (albeit with only positive weights) interacting with CT, which we discuss next.

8.3 Ising spins

The Ising model on a fixed two-dimensional square lattice was first solved by Onsager in 1944. It is very well known to exhibit a second order phase transition between a disordered phase at weak coupling (high temperature) and an ordered phase at strong coupling (low temperature); the scaling limit at the critical coupling is a conformal field theory containing a single Majorana fermion. In contrast, no method to solve the model of Ising spins coupled to CTs is known. Numerical simulations [30] indicate that the effect of the spins on the geometry is weak, and vice versa, so that the critical exponents do not change from the Onsager values and $d_H = 2$; this is corroborated by weak coupling expansions [31], and is also true of the generalization with the 3-state Potts model coupled to CT [32]. There are only a few rigorous results which we now discuss briefly.

For Ising spins on a fixed CT, $G \in \mathcal{C}$, drawn from the ensemble with the measure ρ (48), the existence of a non-magnetised single phase at weak coupling, and multiple phases at strong coupling, was proved in [9]. It was also proved that the critical coupling is almost surely independent of G for such quenched systems. These estimates make extensive use of the tree correspondence. However, they do not easily extend to the CDT case, because then G has to be chosen with a measure $\rho' \neq \rho$ that includes the effect of the spin partition function in the graph weight. This annealed model was studied in [33] where an upper bound on the radius of convergence, expressed as a function of the spin coupling strength, of the grand canonical ensemble was found. It was also shown that at weak coupling the magnetization of the spin at the vertex S_0 on the disk vanishes. Similar results for the annealed q -state Potts model coupled to CTs were obtained in [34]. There is still no proof known to us of the existence of multiple phases at strong coupling in the annealed models.

9 Where next?

As we have seen through this article, there are several outstanding questions concerning CDT, and its extensions with extra degrees of freedom coupled to the geometry, which we draw together here. Firstly, the relationship between the grand canonical ensemble, where only expectation values can be computed, and the infinite graph ensemble, where the graphs dominating the measure have many properties in common, is unclear. The ‘observable’ quantities naturally defined in one differ subtly from those naturally defined in the other. This relationship could be established by the construction of a limiting distribution of continuum surfaces corresponding to the grand canonical ensemble scaling limit. Secondly, much remains to be established for the Ising+CT annealed model. A proof that it magnetises at finite coupling, as seems almost certain from numerical work, would be significant progress; in the infinite graph ensemble this would involve establishing how the measure differs from ρ . Assuming the model does have a continuous phase transition, it would be interesting to establish rigorously whether the critical exponents are shifted from the Onsager values.

Obviously it is of interest to study the CDT model in higher dimensions. In 3 dimensions some progress has been made, see, e.g., [35], and it has been proved that the number of different 3-dimensional CT grows exponentially with the volume so the partition functions one would like to analyse do converge for a range of coupling constants [36]. In 4 dimensions there are essentially only numerical results as described in other contributions to this book. An important outstanding problem is to prove an exponential bound on the number of 4-dimensional CT as a function of volume. In [36] it is shown that such a bound would follow from an exponential bound on the number of unrestricted 3-dimensional triangulations of the sphere, as a function of volume.

Acknowledgements JFW’s research was funded by Research England. BD acknowledges support from Villum Fonden via the QMATH Centre of Excellence (Grant no. 10059). For the purpose of Open Access, the authors have applied a CC BY public copyright licence to any Author Accepted Manuscript version arising from this article.

References

1. J. Björnberg, N. Curien, and S. Ö. Stefánsson, *Stable shredded spheres and causal random maps with large faces*, *The Annals of Probability* **50** (2022), no. 5 2056 – 2084.
2. P. Billingsley, *Convergence of probability measures*. Wiley Series in Probability and Statistics: Probability and Statistics. John Wiley & Sons Inc., New York, second ed., 1999. A Wiley-Interscience Publication.
3. Chassaing, Philippe and Durhuus, Bergfinnur, *Local limit of labelled trees and expected volume growth in random quadrangulation*, *Annals of Probability* **34** (2006), no. 3 879–917.
4. B. Durhuus, *Probabilistic aspects of infinite trees and surfaces*, *Acta Physica Polonica B* **34** (2003) 4795–4811.

5. J. Ambjørn, B. Durhuus and T. Jonsson, *Quantum geometry: a statistical field theory approach*. Cambridge University Press, Cambridge, 1997.
6. P. Flajolet and R. Sedgewick, *Analytic Combinatorics*. Cambridge University Press, Cambridge, 2009. Available at <http://algo.inria.fr/flajolet/Publications/books.html>.
7. B. Durhuus, T. Jonsson, and J. F. Wheeler, *The spectral dimension of generic trees*, *J. Stat. Phys.* **129** (2007) 1237–1260, [arXiv:0908.3643].
8. T. E. Harris, *The theory of branching processes*. Dover Publications, Inc., New York, 2002.
9. M. Krikun and A. Yambartsev, *Phase Transition for the Ising Model on the Critical Lorentzian Triangulation*, *J. Stat. Phys.* **148** (2012), no. 3 422–439, [arXiv:0810.2182].
10. B. Jacquard and G. Schaeffer, *A bijective census of nonseparable planar maps*, *Journal of Combinatorial Theory Series A* **83** (1998), no. 1 1–20.
11. O. Angel and O. Schramm, *Uniform infinite planar triangulations*, *Comm. Math. Phys.* **241** (2003), no. 2-3 191–213.
12. P. Di Francesco, E. Guitter, and C. Kristjansen, *Integrable 2-D Lorentzian gravity and random walks*, *Nucl. Phys. B* **567** (2000) 515–553, [hep-th/9907084].
13. J. Ambjorn and R. Loll, *Nonperturbative Lorentzian quantum gravity, causality and topology change*, *Nucl. Phys. B* **536** (1998) 407–434, [hep-th/9805108].
14. V. Sisko, A. Yambartsev, and S. Zohren, *A note on weak convergence results for infinite causal triangulations*, *Braz. J. Probab. Statist.* **32** (2018), no. 3 597–615.
15. S. Zohren, *A causal perspective on random geometry*. PhD thesis, Imperial Coll., London, 10, 2008. arXiv:0905.0213.
16. B. Durhuus, T. Jonsson, and J. F. Wheeler, *On the spectral dimension of causal triangulations*, *J. Stat. Phys.* **139** (2010) 859, [arXiv:0908.3643].
17. R. Lyons and Y. Peres, *Probability on Trees and Networks*, vol. 42 of *Cambridge Series in Statistical and Probabilistic Mathematics*. Cambridge University Press, New York, 2016. Available at <https://rdlyons.pages.iu.edu/>.
18. T. Coulhon and A. Grigor'yan, *Random walks on graphs with regular volume growth*, *Geom. and Funct. Anal.* **8** (1998) 656–701.
19. T. Coulhon, *Random walks and geometry on infinite graphs*, in *Lecture notes on analysis on metric spaces, Trento, C.I.M.R., 1999* (L. Ambrosio and F. S. Cassano, eds.), Scuola Normale Superiore di Pisa, pp. 5–36, 2000.
20. A. Grigor'yan, *The heat equation on non-compact riemannian manifolds*, *Math. USSR Sb.* **72** (1992) 47–77.
21. W. Feller, *An introduction to probability theory and its applications, Vol. I*. Wiley, London, 1968.
22. L. Breiman, *Probability*. Addison Wesley Publishing Co., Inc., Reading, Mass., 1968.
23. N. Curien, T. Hutchcroft, and A. Nachmias, *Geometric and spectral properties of causal maps*, *Journal of the European Mathematical Society* **22** (2020), no. 12 3997–4024, [arXiv:1710.03137].
24. L. Glaser, T. P. Sotiriou, and S. Weinfurter, *Extrinsic curvature in two-dimensional causal dynamical triangulation*, *Phys. Rev. D* **94** (2016), no. 6 064014, [arXiv:1605.09618].
25. J. L. Cardy, *Conformal Invariance and the Yang-lee Edge Singularity in Two-dimensions*, *Phys. Rev. Lett.* **54** (1985) 1354–1356.
26. M. R. Atkin and S. Zohren, *An Analytical Analysis of CDT Coupled to Dimer-like Matter*, *Phys. Lett. B* **712** (2012) 445–450, [arXiv:1202.4322].
27. J. Ambjorn, L. Glaser, A. Gorlich, and Y. Sato, *New multicritical matrix models and multicritical 2d CDT*, *Phys. Lett. B* **712** (2012) 109–114, [arXiv:1202.4435].
28. J. Ambjørn, B. Durhuus, and J. F. Wheeler, *A restricted dimer model on a two-dimensional random causal triangulation*, *J. Phys. A* **47** (2014) 365001, [arXiv:1405.6782].
29. J. F. Wheeler and P. D. Xavier, *The cylinder amplitude in the hard dimer model on 2D causal dynamical triangulations*, *Class. Quant. Grav.* **39** (2022), no. 7 075004, [arXiv:2109.04414].
30. J. Ambjorn, K. N. Anagnostopoulos, and R. Loll, *A New perspective on matter coupling in 2-D quantum gravity*, *Phys. Rev. D* **60** (1999) 104035, [hep-th/9904012].

31. D. Benedetti and R. Loll, *Unexpected spin-off from quantum gravity*, *Physica A* **377** (2007) 373–380, [[hep-lat/0603013](#)].
32. J. Ambjorn, K. N. Anagnostopoulos, R. Loll, and I. Pushkina, *Shaken, but not stirred: Potts model coupled to quantum gravity*, *Nucl. Phys. B* **807** (2009) 251–264, [[arXiv:0806.3506](#)].
33. G. M. Napolitano and T. Turova, *The Ising model on the random planar causal triangulation: bounds on the critical line and magnetization properties*, *J. Statist. Phys.* **162** (2016) 739–760, [[arXiv:1504.03828](#)].
34. J. C. Hernández, *Potts model coupled to random causal triangulations*, *J. Math. Phys.* **58** (2017), no. 12 123303, [[arXiv:1603.04333](#)].
35. J. Ambjorn, J. Jurkiewicz, R. Loll, and G. Vernizzi, *Lorentzian 3-D gravity with wormholes via matrix models*, *JHEP* **09** (2001) 022, [[hep-th/0106082](#)].
36. B. Durhuus and T. Jonsson, *Exponential Bounds on the Number of Causal Triangulations*, *Commun. Math. Phys.* **340** (2015), no. 1 105–124, [[arXiv:1408.2101](#)].